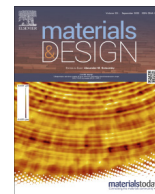


**UCC Library and UCC researchers have made this item openly available.
Please [let us know](#) how this has helped you. Thanks!**

Title	Graphene-based wearable temperature sensors: A review
Author(s)	Nag, Anindya; Simorangkir, Roy B. V. B.; Gawade, Dinesh R.; Nuthalapati, Suresh; Buckley, John L.; O'Flynn, Brendan; Altinsoy, Mehmet Ercan; Mukhopadhyay, Subhas Chandra
Publication date	2022-07-25
Original citation	Nag, A., Simorangkir, R. B. V. B., Gawade, D. R., Nuthalapati, S., Buckley, J. L., O'Flynn, B., Altinsoy, M. E. and Mukhopadhyay, S. C. (2022) 'Graphene-based wearable temperature sensors: A review', Materials and Design, 221, 110971 (17pp). doi: 10.1016/j.matdes.2022.110971
Type of publication	Article (peer-reviewed)
Link to publisher's version	http://dx.doi.org/10.1016/j.matdes.2022.110971 Access to the full text of the published version may require a subscription.
Rights	© 2022, Elsevier Ltd. All rights reserved. This manuscript version is made available under the CC BY-NC-ND 4.0 license. https://creativecommons.org/licenses/by/4.0/
Item downloaded from	http://hdl.handle.net/10468/13542

Downloaded on 2022-12-08T09:08:19Z



Graphene-based wearable temperature sensors: A review

Anindya Nag^{a,1}, Roy B.V.B. Simorangkir^{b,1,*}, Dinesh R. Gawade^b, Suresh Nuthalapati^a, John L. Buckley^b, Brendan O'Flynn^b, Mehmet Ercan Altinsoy^a, Subhas Chandra Mukhopadhyay^c



^a Faculty of Electrical and Computer Engineering, Technische Universität Dresden, 01062 Dresden, Germany

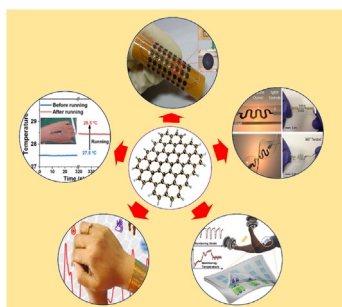
^b Tyndall National Institute, University College Cork, Lee Maltings Complex Dyke Parade, T12R5CP Cork, Ireland

^c Faculty of Science and Engineering, Macquarie University, Sydney, NSW 2109, Australia

HIGHLIGHTS

- The use of various forms of graphene to create wearable temperature sensors is reviewed.
- The manufacturing methods and constituent materials are discussed in depth to provide insight into various development strategies.
- The performance of sensors is analyzed and correlated with the material properties and fabrication methods for a better understanding of the achieved sensor qualities.
- The importance of wireless sensor network in the Internet of Things era is outlined.
- Challenges in graphene-based temperature sensors development are described with potential remedies.

GRAPHICAL ABSTRACT



ARTICLE INFO

Article history:

Received 23 March 2022

Revised 5 July 2022

Accepted 19 July 2022

Available online 21 July 2022

Keywords:

Graphene
Nanocomposites
Nanomaterials
Temperature sensors
Wearable sensors

ABSTRACT

The paper presents a comprehensive review of the use of graphene to develop wearable temperature sensors. The detection of temperature over a wide range has been a growing interest in multidisciplinary sectors in the sensing world. Different kinds of flexible temperature sensors have been fabricated with a range of polymers and nanomaterials. With the additional attribute of wearable nature, these temperature sensors are used ubiquitously to determine the effect of physiochemical variations happening in the environment of the chosen biomedical and industrial applications. Graphene, owing to its exceptional electrical, mechanical, and thermal properties, has been extensively used for the development of wearable temperature sensors. The prototypes have been deployed with certain wireless communication protocols to transfer the experimental data obtained under both controlled environments and real-time scenarios. This paper underlines some of the significant works done on the use of graphene to fabricate and implement wearable temperature sensors, along with the possible remedial steps that can be considered to deal with the challenges existing in the current literature.

© 2022 The Author(s). Published by Elsevier Ltd. This is an open access article under the CC BY license (<http://creativecommons.org/licenses/by/4.0/>).

* Corresponding author.

E-mail addresses: anindya1991@gmail.com (A. Nag), roy.simorangkir@tyndall.ie (R.B.V.B. Simorangkir), subhas.mukhopadhyay@mq.edu.au (S.C. Mukhopadhyay).

¹ These authors contributed equally to this work.

1. Introduction

There has been a growing interest in the use of sensors for improving the quality of human life for the last two decades. Scientists have constantly been trying to improve the quality of the sensors in terms of sensitivity, accuracy, and longevity for the chosen applications. In earlier times, when semiconducting sensors got popularized [1–3], prototypes were mostly developed using silicon substrates due to their small size, low hysteresis and ability to work in harsh environments [4–6]. These sensors were mostly fabricated using the microelectromechanical systems (MEMS) technique. Although these sensors were used for different kinds of industrial [7–9] and environmental [10–12] applications, there are limitations that needed alternative options. This led to the development of sensors with flexible materials having enhanced electrical, mechanical, and thermal characteristics [13–15].

Such sensors were fabricated using different kinds of contact and non-contact printing techniques, including screen printing [16–18], inkjet printing [19–21], 3D printing [22–24], and laser cutting [18,25,26] processes. These fabrication techniques have been used to a large extent to process flexible polymers and conductive nanomaterials. Among the polymers, some of the common ones that have been used to form the flexible sensors are polydimethylsiloxane (PDMS) [27–29], polyethylene terephthalate (PET) [30–32], and polyimide (PI) [33–35]. Each of these polymers differs in terms of mechanical, electrical, and thermal characteristics. In recent days, conductive polymers like PEDOT: PSS [36–39] have also been used to avoid the reduction in the electrical conductivity while forming composites for the electrodes of the flexible sensors. All these polymers have been used individually or in the form of nanocomposites by mixing them with different kinds of nanomaterials at defined proportions. The choice of nanomaterials is typically made based on the application chosen for the sensors. For instance, sensors intended for biomedical applications, need to consider biocompatibility, hydrophobic, higher sensitivity and possibly, minimal pre- and post-processing steps. The commonly used nanomaterials can be broadly classified under two categories: carbon-based allotropes and metallic nanomaterials. The former category includes Carbon Nanotubes (CNTs) [40–42], graphene [43–46], and graphite [47–50], while the latter includes nanoparticles based on gold [51–54], silver [55–57], aluminum [58–60], and copper [61–63]. With the use of the aforementioned fabrication techniques and materials, it has been possible to develop sensors with wearable nature, thus can be applied to the human body with minimum to no discomfort even for prolonged use. Such wearable sensors have been advantageous for their capability to increase the quality of life at a lower cost [64–66].

Temperature is one of the most important human physiological parameters that can be used as a reference value for health-related problems monitoring. Accurate and precise measurement of body temperature is, therefore, very essential. Despite the high resolution and accuracy of measurement, commercially available contact-based temperature sensors are typically rigid, which raises concerns about their suitability for prolonged on-body usage [67], for instance, in the context of real-time health monitoring system. It is also challenging for such sensors to perform localized temperature measurements in curved surfaces of the body, let alone to distinguish signals from the skin's surface without impeding the users' mobility. Infrared (IR) devices and thermal imaging cameras seem to provide a fast non-contact solution to the above. However, a line of sight with the object under test must be maintained, as well as awareness of the surface's emissive qualities. This motivates the development of wearable temperature sensors capable of monitoring dynamic and spatial variations in temperature. To

comply with on-body operation and so give a viable solution to the above, wearable sensors are desired to be flexible, stretchable, biocompatible, highly sensitive, lightweight, and physically durable. Several types of flexible temperature sensors have been reported in recent decades, including thermocouple [68,69], thermoresistance [70,71], and thermal-responsive field-effect transistor-based temperature sensors [72–74]. However, since these sensors have exhibit a narrow thermal dynamic range, they typically require complicated electronic circuits to ensure accurate detection, which makes their implementation for wearable applications challenging [75]. Patterning temperature sensitive materials on sheet-like flexible/stretchable substrates is the most frequent method for developing wearable temperature sensors. Pure metals such as platinum, gold, nickel have demonstrated a linear change in resistance as a function of temperature [67,70] and a good temperature coefficient of resistance (TCR), typically in the range of 0.3–0.6%/°C [76]. These metals, however, often need a high processing temperature, making them costly and difficult to work with [76,77] and even incompatible with certain heat-sensitive flexible substrates [67].

Out of the nanomaterials listed earlier, graphene has been one of the most influential elements in forming efficient, flexible sensors due to its exceptional electrical, physical, thermal and chemical properties [78,79]. Graphene is a carbon monolayer with a honeycomb lattice. The physical characteristics of graphene have been intensively investigated since its isolation from graphite by the micromechanical cleavage technique in 2004 [80]. Some of the particular traits including large specific surface area, high electron mobility, high tensile strength, flexibility, transparency, and biocompatibility, have led the researchers to opt for graphene as a stimuli response material for different sensing applications [79,81,82]. Among these superior properties, it is the outstanding thermal conductivity of graphene (i.e., higher than metals and CNTs [83]), together with its excellent mechanical and electrical properties, as well as its unique temperature-responsive properties, that renders it a great candidate for temperature sensing applications [84–86]. From a fabrication standpoint, due to the electromechanical properties of graphene, its integration with substrate materials is also relatively easier compared to metallic nanomaterials.

In this paper, we present a comprehensive review of the use of graphene to construct wearable sensors for temperature sensing applications. There have been a lot of review papers written in the context of graphene and its implementation for sensing applications. For example, comprehensive reviews on the synthesis, characterization, properties, as well as a wide range applications of graphene can be found in [87–92]. Nag et. al in presents a broad overview of graphene for sensors development in [43]. Other researchers, on the other hand, provide a technical overview of graphene for more specific applications, such as chemical and biological sensing [93–95], strain sensing [44,96,97], gas/vapor sensing [98,99], and human health monitoring [100]. To our knowledge, a review of the application of graphene for wearable temperature sensors development, which is the focus of this paper, has yet to be reported.

The presentation of this paper has been divided into three parts. We start the review by providing different variants of graphene that have been employed for temperature sensing applications (Section 2). For each variant, we provide some examples, along with the details on the employed materials, fabrication techniques, and the performance of fabricated sensors correlated with the composing materials, manufacturing strategies, and sensing principle, to name a few. The third section summarizes key performance indicators of temperature sensors comparing graphene-based and

non-graphene-based sensors published in the literature to date. The fourth section describes the wireless network scenario for continuous sensing and monitoring of the developed sensors. In the fifth section, we explain the challenges faced by the current wearable temperature sensors along with some possible remedies. The conclusion of the paper is drawn in the final section of the manuscript.

2. Graphene taxonomy and its implementation for temperature sensor

Graphene, the building block of many carbonic materials, is a two-dimensional crystalline material made of a basal monolayer of sp^2 hybridized carbon atoms, joined together in a hexagonal honeycomb structure. Although graphene was theoretically predicted long ago [101], it was only actually produced in 2004 [80]. In its traditional form, graphene is one atomic thick and generally exists as a film of sorts. The proliferation of graphene research and testing, however, has resulted in its implementation in various forms. These wide ranges of graphene materials have been employed to produce temperature sensors in conjunction with different types of materials to exhibit unique engineering qualities and sensing capability. Such integrations were achieved through a variety of manufacturing approaches considering the state of the constituent materials as well as the target performance of the temperature sensing system. In this section, we discuss different forms of graphene that have been employed for the realization of temperature sensor together with some relevant substantial works.

2.1. Graphene oxide-based temperature sensors

Graphene oxide (GO) refers to the oxidized variant of graphene. GO has a 2D structure similar to graphene, but the single-layer of carbon atoms is covalently functionalized with oxygen-containing groups (such as hydroxyl, carbonyl, and epoxide, to name a few) above and below the sp^2 C basal plane [102]. By removing the oxygen functional groups from its surface, its physical characteristics can be varied from those of fully oxidized GO to those of graphene. Unlike graphene, due to the presence of the oxygen functional groups, GO is hydrophilic and can be dispersed in water to form single-layer GO solutions [102]. GO flakes are typically irregular in size, but they can be easily tuned from a few nm to mm scale, for instance, via sonification. Owing to the GO's chemical composition and flakes size tunability, GO is seen as a promising material for a variety of applications, including renewable energy device, biology, medicine, and electronics. With the huge number and diversity of functional groups on GO's surface, which may serve as potential anchoring sites for a range of molecules, GO is intrinsically a good material particularly for gas sensing or biosensing. However, the dielectric nature of GO, which prevents an efficient extraction of the electric signal from the sensor, hinders its popularity.

In [103] Hou et al. presented a dual strain-temperature sensor based on sodium alginate (SA) nanofibril/GO/polyacrylamide (PAM) nanocomposite hydrogel, denoted as SNGP hydrogel. The strong entanglement of the alginate nanofibril and PAM networks contributed to the remarkable mechanical properties of the SNGP hydrogel. The addition of GO as a strengthening agent and thermal conductor, on the other hand, gave the hydrogel improved mechanical characteristics and thermal sensitivity. The SNGP nanocomposite hydrogel was made by mixing a prepared and incubated SA/NaCl solution with GO, monomer, cross linker, accelerator and thermos-initiator, followed by curing for 3 h at 50 °C. The SNGP nanocomposite hydrogel was encapsulated in a PET film or VHB tape to create the sensor. The constructed sensor showed a

negative temperature coefficient of resistance (TCR) with a sensitivity of 2%/°C within the temperature range of 25–65 °C (Fig. 1 (a) and (b)). The resulted sensitivity value was higher than that of typical ionic hydrogel-based sensors, possibly as the result of the electron hopping at the neighboring graphene sheets interface [104]. With an increase in strain from 0% to 200%, this temperature sensitivity rose from 2.0%/°C to 2.7%/°C (Fig. 1(c)), which might be associated with increased structural disorders of the graphene under pressure [105]. Apart from that, the sensor exhibited a high tensile strength (0.54 MPa), excellent stretchability (3370%), and a high compression strength (4.4 MPa). The study discovered that increasing the GO content increased the toughness of the developed sensor. As a strain sensor, it exhibited a GF of 4.2 at a tensile strain of 2000% and can detect an exceptionally small strain of 0.02% at a low voltage of 0.5 V. The excellent electric property of GO was responsible for the latter's enhanced sensitivity.

Ren et al. developed capacitive-temperature sensors employing GO in [106]. The devices consisted of a planar coil and temperature-sensitive capacitor forming an LC tank whose resonant frequency was a function of temperature. GO films, used as the sensing layer, was synthesized using the modified Hummers method, followed by exfoliation through ultra sonication process. Fig. 2(a) shows the schematic diagram of the fabrication process of the GO-based wearable temperature sensors. Initially, p-type silicon wafers were flip-chipped onto glass wafers using an anodic bonding process, which was further processed with a chemical mechanical planarization process. The samples were then trenched using the inductively coupled plasma technique, followed by attaching the FR-4 substrate-based interdigitated temperature-sensitive capacitors with an adhesive layer. Finally, spiral copper inductors were attached to the same substrates using a standardized printed circuit board (PCB) process. Wire bonding was employed to make the electrical connection between the capacitor and the inductor on the substrate. As part of the device, a telemetric unit consisting of an antenna analyzer and a readout coil was interfaced to the sensing unit through an electro-magnetic coupling for characterization purposes. The resonant frequency of the system, which changed as a function of temperature, thanks to the GO, was monitored through the impedance change captured by the antenna analyzer. With the increase in temperature, the peak of the real impedance shifted to lower frequency (Fig. 2(b) and (c)). Sensitivities of 59.3 kHz/°C and 46.1 kHz/°C were obtained in temperature ranging from –40 °C to 0 °C and from 10 °C to 60 °C, respectively.

2.2. Reduced graphene oxide-based temperature sensors

Reduced graphene oxide (rGO), another derivative of graphene, is produced when further reductive exfoliation treatment is applied to GO. The reduction of GO can be done through various ways, e.g., chemical, thermal, microwave, and electrochemical. The diversity of the process and the degree of reduction may result in rGO of varying grade [107]. Having less oxygen functional groups, rGO exhibits properties that are more similar to those of pristine graphene, such as greater electrical conductivity and carrier mobility as compared to GO. The graphene-like properties of rGO have made it an attractive material for the development of nano/hierarchical devices for various applications, including batteries, optoelectronics, supercapacitors, membranes, catalysts, absorbers, anticorrosion, lubricants, and flexible sensors [107].

One interesting example employing rGO is the work done by Liu et al. [108]. The researchers showcased the use of rGO for the development of temperature sensors suitable for robot skin and the internet of things (IoT). In this effort, rGO was sandwiched between a high-temperature transparent tape acting as an insulating layer and a PET substrate. The sensor was fabricated and compared with other sensors with the same configuration but using

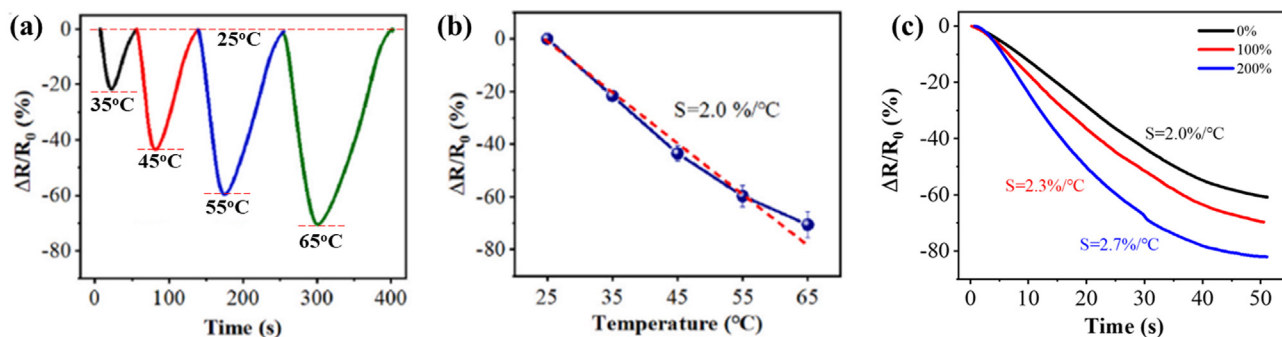


Fig. 1. Performance of SNGP hydrogel-based strain-temperature in [103]: (a) dynamic resistance response as the temperature changes from 25 °C to 35 °C, 45 °C, 55 °C, and 65 °C, (b) relative resistance change as a function of temperature, and (c) relative resistance change under different strains when temperature changes from 20 °C to 55 °C. Reproduced from [103] with permission. Copyright (2021) Elsevier Ltd.

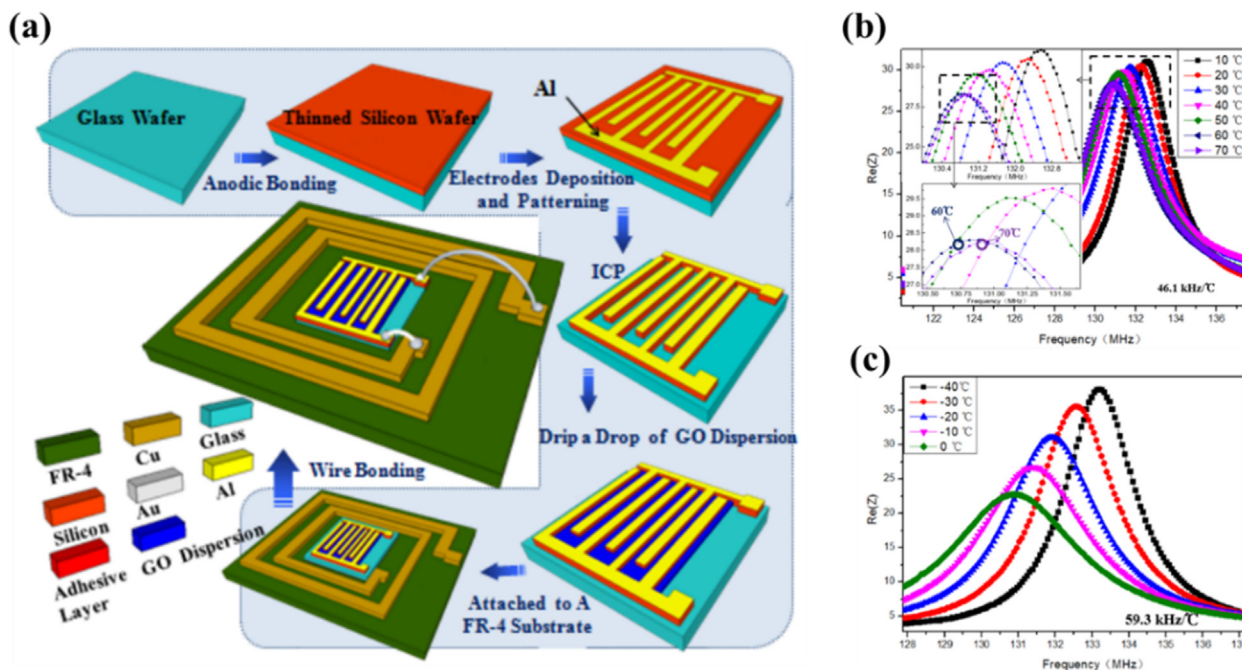


Fig. 2. (a) Fabrication process of GO-based temperature sensors in [106]. (b) Measured real impedance of the system as temperature changes from 10 °C to 60 °C. (c) Measured real impedance of the system as temperature changes from -40 °C to 0 °C. Reproduced from [106] with permission. Copyright (2014) IEEE.

single-walled carbon nanotubes (SWCNTs) and multi-walled carbon nanotubes (MWCNTs) as the sensing layer. Plasma etching was involved in the fabrication process to build irregular microstructures on the surface of the PET to improve the attachment of the carbon sensing layers on the substrate. The screen printing process was also utilized to fabricate two conductive thin wires. Fig. 3(a)–(h) show the schematic diagram of the fabrication process of these sensors along with the fabricated sensors. As shown in Fig. 3(i)–(k), the resistance response of the rGO and MWCNTs-based sensors was linear with temperature, whereas the SWCNTs-based sensor was nonlinear. All prototypes exhibit a negative TCR with the rGO-based prototype showing the highest sensitivity of 0.6345%/°C. Another advantage of the developed rGO sensor was its durable mechanical qualities, which allowed the resistance of the sensor to remain largely stable even when subjected to various pressures and deformations. This was accomplished by reducing the space between the graphene layers by applying a high force when adhering the insulating layer. The insulating layer also rendered the sensor resilient to changes in surrounding humidity and other gases.

Another interesting work is shown by Sahatiya et al. [109]. rGO was used as a channel that bridged the electrodes fabricated over a PI substrate, resulting in a flexible and transparent temperature sensor. Another version of the sensor using commercial graphene flakes was also developed. The graphene solutions were both drop-casted, while the electrodes were made out of copper through the microfabrication technique. The fabricated sensors were subsequently tested for their performance for both infrared sensing and temperature sensing. Within the temperature of 35 °C and 45 °C, the sensors showed TCR values of -0.7429%/°C and -0.413%/°C for the rGO and graphene flakes, respectively, both indicated a higher sensitivity than a commercially available platinum-based temperature sensor (TCR of 0.39%/°C) [110]. The vast number of thermally activated defect traps present in rGO, which contributed to long range variable hopping of the electrons, may be the cause of the high sensitivity of this rGO-based sensor [111]. This was in addition to having a larger activation energy (i.e., 90.7 meV) than the graphene flakes-based sensor (i.e., 24.19 meV). Similar work on the use of rGO for developing wearable temperature sensors can be seen in [112]. But here, the fabri-

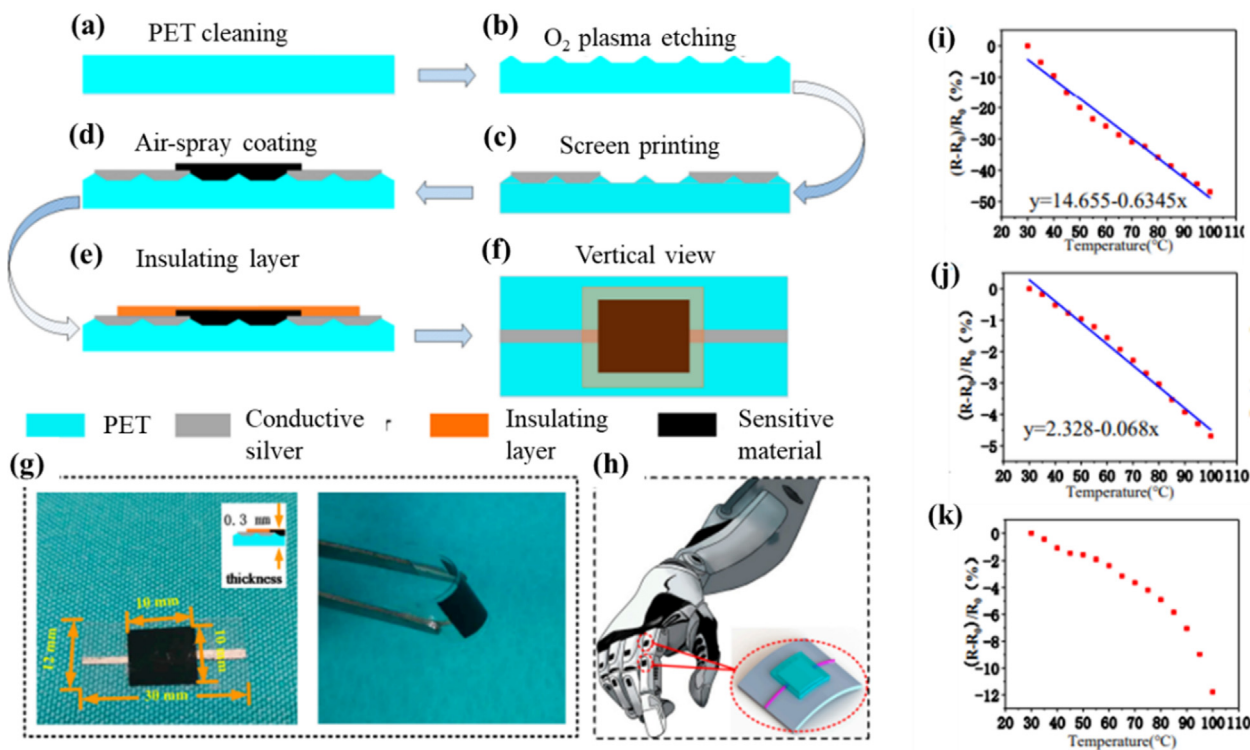


Fig. 3. (a)–(f) Fabrication process rGO-based flexible temperature sensors in [108]. (g) Structural dimensions of the sensors. (h) Implementation of the fabricated sensors on robot skin. (i)–(k) Relative resistance changes for rGO, MWCNTS, and SWCNTS, respectively, as temperature changes from 30 °C to 100 °C. Reproduced from [108] under a Creative Commons Attribution 4.0 International License (CC BY 4.0). Copyright (2018) The Authors.

cation approach was different since the rGO was drop-casted directly on platinum interdigital electrodes, followed by low-temperature annealing and hydrazine vapor treatment. The resistance decreased exponentially as the temperature increased from 100 K to 400 K. Above 240 K, the resistance response was almost linear with a TCR of $-0.38\%/K$. The sensors exhibited some other attributes like high sensitivity, stability, and repeatability. The behavior of the sensors was comparable to that of a standard temperature controller.

Zhang et al in [113] developed a multi modal strain and temperature sensor through hybridization of PEDOT:PSS and rGO in an aerogel form and infusing it with PDMS. The PEDOT:PSS/rGO aerogels were made by freeze-drying a mixture of PEDOT:PSS and GO nanosheets synthesized using a chemical reduction-induced self-assembly technique. The prepared aerogel was then mixed with PDMS precursor, which infiltrated into the pores of the aerogel, resulting in a stretchable strain sensor. Exhibiting positive and negative sensitivity to strain and temperature, respectively, this sensor can identify both stimuli using an impedance technique. By measuring the electrical impedance of the sensor at two distinct frequencies, both strain and temperature may be easily calculated with just one sensor. The gauge factor of the sensor created with the PEDOT:PSS/rGO/PDMS nanocomposite at a weight ratio of 1:30 and a total filler concentration of 2.5 mg/ml was found to be approximately 57.6. The developed sensor displayed decreasing resistance as the temperature increased with a TCR of $-1.69\%/^{\circ}C$ in the temperature range of 30–50 °C.

Dan et. al described the design, fabrication, and characterization of temperature sensors employing conductive polymer composite (CPC) and rGO in [76]. The response of a CPC-based composite may result from the temperature-dependent properties of the polymer itself or nanofiller. The polymer and nanofiller's temperature-dependent effects may conflict with one another (for example, when the polymer has a positive TCR while the nano-

filler has a negative TCR), resulting in a weak or non-linear electrical behavior. In this study, the authors formed a nanocomposite ink using biopolymer polyhydroxybutyrate (PHB) as the polymer matrix and sheet-like rGO (from 3 to 12 wt%) as the nanofiller (Fig. 4(a)). Because PHB exhibited a relatively small thermal expansion, rGO's temperature-dependent characteristics dominated the composite's overall response, thus addressing the above issue. The room temperature resistivity, as well as the temperature-dependent resistance of this composite, were greatly determined by the rGO's weight percent loading. Below the percolation threshold (i.e., 3 wt%), the composite was typically insulating and exhibited minimal change in resistance as a function of temperature. Above the threshold, the conductivity, the Hall mobility and charge carrier density of the composite increased significantly. The composite was also moderately conductive and had minor but steady and repeatable resistance decrease upon heating, just like pure rGO. The temperature sensor was fabricated by drop coating the PHB-rGO composite ink on inkjet-printed silver electrodes or direct ink writing (DIW) the ink on flexible and stretchable substrates such as PET and PDMS (Fig. 4(b) and (c)). The TCR value of the PHB-rGO-based sensor with 3 wt% loading (the highest responsiveness of all composites) was $-0.8\%/^{\circ}C$ within 20 °C and 65 °C (Fig. 4 (d)). The TCR absolute value was comparable to that of nickel (i.e., $0.6\%/^{\circ}C$) [76], validating its potential for temperature-sensing devices. This composite was also water-resistant due to the hydrophobicity of its the polymer matrix. This allowed the developed sensor to be used for monitoring temperature profiles in wet situations, such as within the body or underwater.

2.3. Graphene nanoplatelets-based temperature sensors

Graphene nanoplatelets (GNPs) are stacks of platelet-shaped graphene sheets, which are comparable to those seen in the walls of carbon nanotubes but in planar form. They are also known as

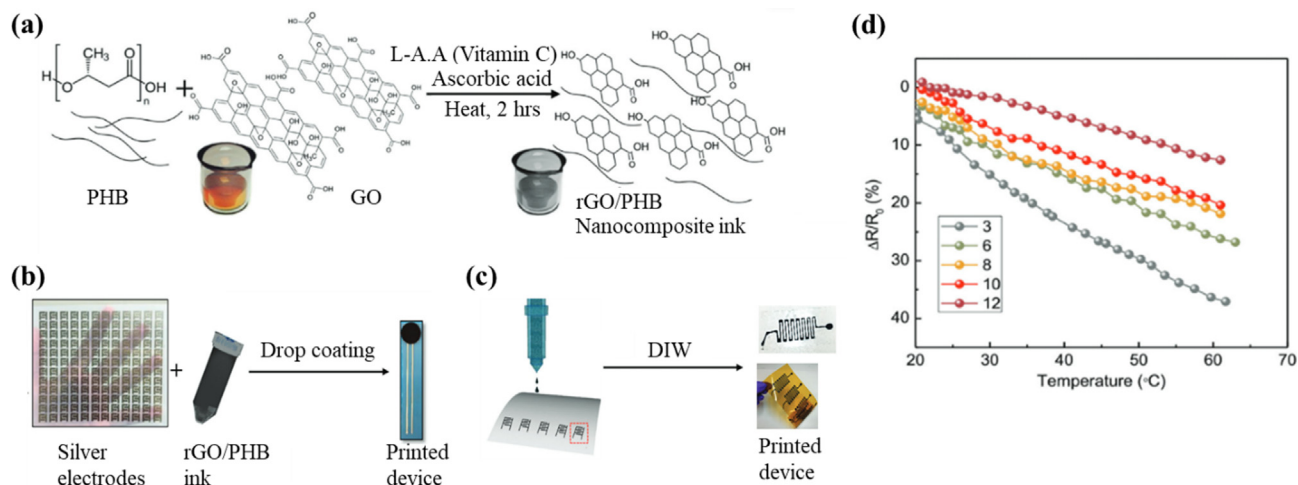


Fig. 4. (a) In-situ reduction for preparation of rGO/PHB nanocomposite ink in [76]. Sensors fabrication through (b) drop-coating and (c) direct ink writing (DIW). (d) Temperature-dependent response of drop-coated sensor with varying rGO loading (i.e., 3–12 wt%). Reproduced from [76] with permission. Copyright (2020) The Authors.

graphite nanoplatelets since they contain of more than 10 graphene layers [114]. GNPs typically range from 50 to 750 m²/g in surface area and 5 to 10 nm in thickness. They may be produced in sizes ranging from 1 to 50 μm. Their key characteristics include lightweight, good mechanical properties, great thermal and electrical conductivities, high aspect ratio with planar shape, together with low cost and easy manufacture (unlike pristine graphene). Due to their appealing powder or granular shape, which can be quickly and effectively incorporated into the polymer matrices by solvent and melt counteracting, they are the preferred material for advanced nanocomposites. In most cases, the inclusion of GNP enhances barrier properties and thermal conductivity, improves mechanical and tribological performance, turns insulating matrices into electrical conductors, and works as a flame retardant. While less chemically reactive than GO, GNPs are similarly effective as tube-like nano-fillers in modifying the chemical properties of polymers as well as safer than carbon nanofibers and nanotubes.

A 3D printing technique of GNPs/PDMS inks was employed in [115] to develop nanocomposite-based sensors that were stretchable and strain-insensitive. Through a solvent bending approach, the authors successfully developed nanocomposite inks with shear-thinning rheological behavior suitable for a smooth and stable 3D printing process. Fig. 5(a) shows the fabrication steps of the nanocomposite inks. Graphene flakes were used as the precursor material, which was processed to form the intercalated graphite compound. These compounds were annealed at 1050 °C for 25 s to form GNPs. The GNPs were then mixed with ethyl acetate and then with PDMS to form the nanocomposite inks. The shelf life of the inks was around 60 days at a temperature of 4 °C. The sensors were fabricated with various cellular architectures (i.e., grid, triangular, and hexagonal) apart from solid using a 3D direct ink-writing printer connected to a computer-controlled 3D movement platform. The printed prototypes were cured at 150 °C for 1 h before removing them from the printing platform and using them for characterization and experimental purposes. Through optical observations of the printed structures, it was confirmed that the nanocomposite inks allowed for long-range-ordered and precisely controlled porous cellular structures. The experiments were conducted for a temperature ranging between 25 °C and 75 °C. The sensors displayed a positive TCR with a sensitivity of 0.8%/°C (Fig. 5(b)) which was higher than that of standard commercial platinum-based temperature sensor (i.e., 0.39%/°C) [110]. The range of response and recovery times of the sensor with grid por-

ous structure were 1.31–3.91 s and 1.01–4.58 s, respectively, indicating a better performance than the platinum sensor. The sensitivity of the sensors as a function of deformation was also investigated. In general, the sensors with long-range-ordered porous structures (i.e., grid, triangular, and hexagonal) demonstrated better temperature sensitivity under stress (Fig. 5(c)), which was understandable given that the fine porous structure can effectively share the external strain, thus resulting in a more stable electrical resistance and reduced effect of strain on the temperature-sensing properties [116]. This feature was significantly important for real-time applications on curved or complicated structures, for instance the human body.

2.4. Graphene nanowalls-based temperature sensors

Graphene nanowalls (GNWs), also known as carbon nanowalls, carbon nanosheets, and carbon nanoflakes, are a class of graphene networks that consists of graphene nanosheets forming self-assembled vertically standing wall structures on a substrate [117]. Each nanosheet typically consists of 1–10 layers of graphene with an interlayer spacing of 0.335 nm. The wall structures typically have thickness varying from a few to a few tens of nanometers and have a high aspect ratio. Due to its high density of atomic size graphitic edges, GNWs have generated a lot of attention for prospective use as light sources and flat panel displays. The large surface area of GNWs offers great promise for the development of batteries, capacitors, and sensors [117,118]. In these applications, metal nanoparticles and other elements are often added.

Wei et al. [75] showed the use of GNWs and PDMS to develop wearable temperature sensors. The sensors were fabricated by employing plasma enhanced chemical vapor deposition (PECVD) technique and polymer-assisted transfer method. The procedure began with the synthesis of GNWs on copper foils using a low pressure RF PECVD technique. This was followed by a series of polymethylmethacrylate (PMMA)-free transfer processes, which helped to preserve the GNW's vertical morphology, crucial for a high temperature sensitivity. The connections of the prototypes were formed using silver paste at both ends of the sensor. Measured from 35 °C to 45 °C, the developed sensor exhibited a positive TCR of 21.4%/°C which was 2 orders larger than that of standard commercial platinum temperature sensors (i.e., 0.39%/°C) [110]. As the temperature rose, the radial expansion of the PDMS substrate stretched the interlaced GNWs network into a

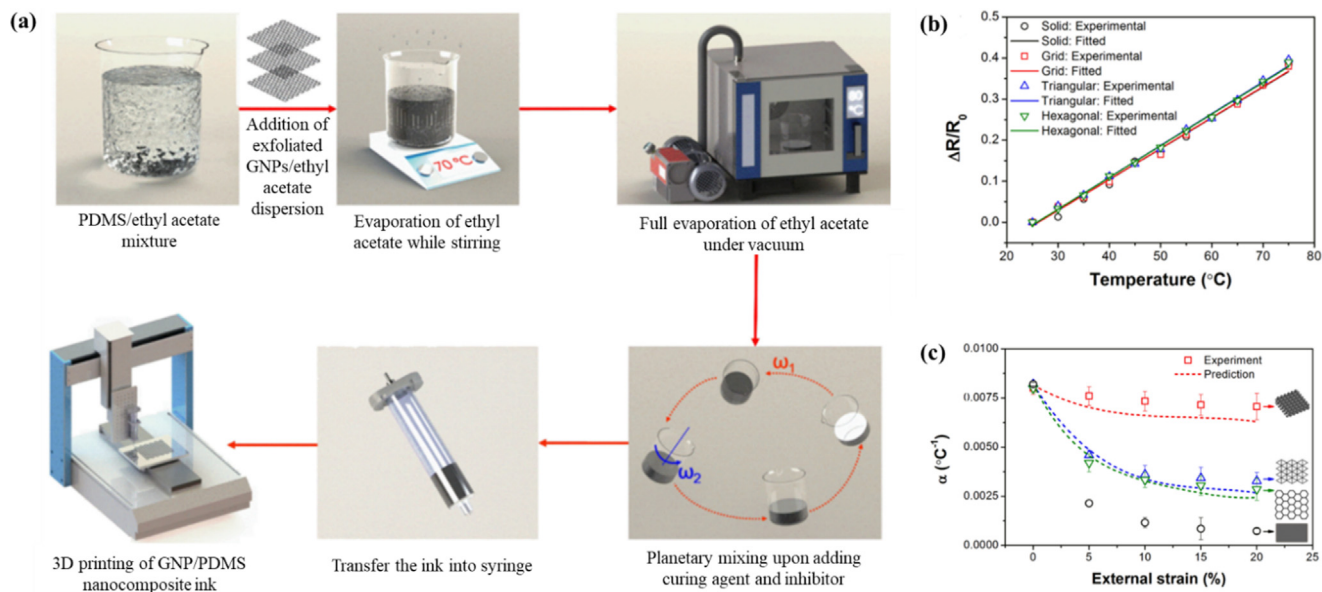


Fig. 5. (a) Preparation of the GNP/PDMS nanocomposite inks for 3D printing of the sensors in [115]. (b) Resistance response of the fabricated sensors as a function of temperature from 25 °C and 75 °C. (c) Temperature sensitivity of the sensor as a function of external tensile strain. Reproduced from [115] with permission. Copyright (2018) American Chemical Society.

loose conductive network, and the very high thermal expansion coefficient of PDMS caused fractures to occur. As a result, compact graphene nanosheets generated much longer conducting channels between the two electrodes, which explained a large increase in resistance and the very high thermal responsiveness above. On other note, the conductive channels reverted to their initial state upon cooling, suggesting a fully recoverable conductive channel throughout the thermal expansion and contraction of the PDMS, resulting in exceptional stability.

2.5. Laser-induced graphene-based temperature sensors

Laser-induced graphene (LIG) is a class of 3D porous carbon nanomaterial which is composed of a percolating network of porous multilayer graphene. LIG may be formed by subjecting a variety of carbon precursors, such as PI, poly(ether sulfone), wood, food, clothes, and paper, to mention a few, to laser irradiation in an ambient environment [119]. The photo-thermal production of graphene results from the local heating induced by the laser irradiation of the carbon precursors. The C–O, C=O, and C–N bonds are easily destroyed by the high temperature, which is confirmed by the significantly reduced oxygen and nitrogen levels in LIG. LIG offers a variety of benefits and prospects as it not only possesses electrochemical properties of graphene, but also has higher specific surface area. In contrast to conventional graphene manufacturing approaches, such as thermal decomposition, mechanical stripping, epitaxial growth, CVD, and wet chemical methods, LIG is unique as it can be completed in a single step at a lower cost and with less negative environmental impact [120]. The graphene size, morphology, and texture can be easily controlled through laser writing or engraving, process parameters without any additional step. This controllable fabrication, design, and texture of LIG via computer-based systems hold a great promise toward printable electronics for sensing based applications.

Marengo et al. [121] showed one of the interesting works employing LIG for developing flexible temperature sensor. Carbonization was done on a PI substrate using CO₂ lasers, where optimization was done on various laser parameters, including wavelength, power, speed, working distance, and pulse per inch.

The contact pads were formed using copper tape connected to LIG tracks by silver paint. The temperature sensors displayed with a decrease of resistance values by 4% when the temperature increased from 20 °C to 60 °C, or similarly a TCR of $-0.1\%/^{\circ}\text{C}$. Similar work was reported in [122] where a LIG-based sensor was developed through a straightforward CO₂ laser irradiation of a PI film. To ensure accuracy, hydrosol and double-sided tapes were incorporated and the process was done over an acrylic board as shown in Fig. 6(a). At the end of the process, the hydrosol tape was dissolved in clean water and the resultant sensor can be detached from the acrylic board safely. The sensor temperature response was characterized between 30 °C and 40 °C, simulating the human body temperature limit, and a TCR of $-0.04145\%/^{\circ}\text{C}$ was observed (Fig. 6(b)). The sensor response might be affected by the contradictory thermal coefficients of LIG and PI [121].

2.6. Graphene textile-based temperature sensors

Over the last several years, the textile industry has seen significant growth and innovation. Modern textiles no longer qualify as mere clothing since nowadays they incorporate new functionalities, including electrical conduction, UV protection, flame resistance, electrochromic, thermal regulation, self-cleaning, antimicrobial, solar energy harvesting, photonic, or even catalysis. These functionalities are normally provided by the development and implementation of new materials. Having mentioned all the qualities and potentials of graphene materials family, the incorporation of graphene into textiles is a natural step to do. Not only graphene can enhance resistance to wear, abrasion, and tearing, it also can increase thermal and electrical conductivity, which all open up opportunities for smart textiles for various applications.

In [123], for instance, Afroj et al. developed rGO based graphene inks suitable for highly scalable and ultrafast yarn dyeing technique for the production of graphene textile-based temperature sensors. This was done by engineering the formulation and reduction conditions of rGO flakes. GO was initially synthesized with the modified Hummers method and chemically reduced to rGO through a modified reduction process which involved ascorbic acid (AA) and sodium hydrosulfite (SH) as reducing agents and opti-

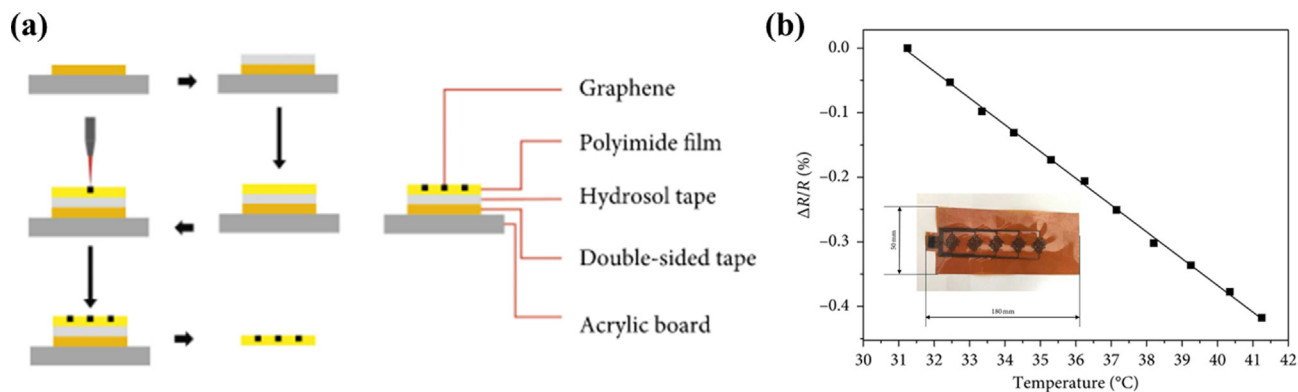


Fig. 6. (a) Fabrication of the LIG-based temperature sensor in [122]. (b) Thermal-dependent resistance of the developed sensor as temperature changes from 30 °C to 40 °C. The inset shows the fabricated LIG-based sensor. Reproduced from [123] under a Creative Commons Attribution 4.0 International License (CC BY 4.0). Copyright (2021) The Authors.

mized reduction time and temperature. Poly(sodium 4-styrene sulfonate) (PSS) and poly(vinyl alcohol) (PVA) were added to functionalize the rGO flakes surface to have better dispersibility and prevent agglomeration. Yarn dyeing techniques, i.e., dip coating and exhaust dyeing, were then employed to produce rGO-coated yarns, which were further transformed into textile sensor structure through an automatic knitting process. The temperature sensitivity and hence usability of the produced inks were validated through testing of the temperature-dependent conductance for individual rGO flakes, overlapping rGO flakes, drop-casted rGO films, and free-standing rGO-coated yarns (Fig. 7(a)–(c)). The findings also indicated that rather than the transport across flakes, the conductivity of individual flakes had a substantial role in determining the temperature sensitivity. Experimental investigations were conducted to optimize some key parameters of the dyeing process, such as coating time, number of coating cycles, curing time and temperature. It was discovered that the resistance of rGO-coated yarn decreased with the increase of coating time. The resistance followed the same trend when the number of the coating cycle increased, which was anticipated given the rise in the quantity of rGO flakes deposited on the yarn surface. The resistance decreased significantly with the increase in curing temperature and time due to the volatilization of the residual solvent. It was also observed that a high curing temperature reduced the contact resistance of the rGO flake network, enabling a more efficient charge transport. Wash stability testing was also conducted. The research revealed that when compared to graphene flakes-coated yarn, the rGO-coated yarn had better wash stability. Confirmed through X-ray photoelectron spectroscopy (XPS) analysis, this behavior was caused by the oxygen functional group of rGO, which formed covalent or hydrogen bonding with the fibers and improved wash stability. To achieve a graphene-coated yarn-based temperature sensor with the most robust knitted scaffold, the sensor was built using an interlock construction of double-covered yarn with a Lycra filament core and a nylon filament covering (Fig. 7(d)). The sensors depicted repeatable results in terms of electrical resistance for cyclic tests done between 25°C and 55°C exhibiting a linear negative TCR (Fig. 7(e)).

Motivated by an interest to develop temperature sensors that can be fully integrated into textile, allowing for more seamless integration of the sensing system into the users' clothing, Rajan et al. developed graphene-coated polypropylene (PP) monofilament textiles that can perform as a resistive temperature sensor [67]. Several graphene films were prepared: three types were grown through CVD (i.e., single-layer graphene (SLG), trilayer graphene (TLG) grown on copper, and few-layer graphene (FLG) grown on nickel) and one type was grown through shear exfolia-

tion of graphite (SEG). The sensors were developed by coating the PP textiles with the prepared graphene films. Carbon paste and silver ink were compared for their suitability as the sensor contact points to facilitate the measurements. The developed sensors were almost invisible due to its small dimension and optical transparency, which led to easy and seamless integration into garments. The performance of all fabricated sensor was determined in terms of the change in resistance with respect to the temperature change from 30 °C to 70 °C. There was no sign of temperature-dependent resistance in the FLG-based sensor, indicating that this form of graphene may not be suited for temperature sensing possibly due to the larger number of layers. The SLG and SEG-based sensors, on the other hand, showed some temperature sensitivity but were not reproducible. It was believed that single layer graphene was too thin to withstand temperature cycle. In addition, for the case of SEG-based sensor, the SEG film was composed of overlapping graphene flakes rather than merging crystalline domains and it contained the residues of the surfactant required during the process. All of this explained the unreliability of the SLG- and SEG-based sensors. In the instance of the TLG-based sensor, a negative temperature coefficient behavior with a TCR of $-0.17\%/^{\circ}\text{C}$ within a temperature range of 30–45 °C was observed, which was highly stable over ten temperature cycles (Fig. 8(a)). Carbon paste was found to be the best option for the contact points. The mechanical stability and washability tests of the TLG-based sensor revealed no substantial change in its sensitivity (Fig. 8(b) and (c)). In addition to being washable and lightweight, the sensor can also operate at voltages as low as 1 V.

Wang et al. showcased another approach of developing graphene-fabric resistive temperature sensors in [124]. The sensor was developed through a simple dip-coating of a non-woven fabric into GNPs that was dispersed by sodium alginate with optimized concentration. The non-woven fabric was prepared through a wet-spinning process of calcium alginate fibers. Fig. 9(a) and (b) shows the illustration of the wet spinning and dip-coating processes involved in the development of the temperature sensor. The mechanical properties of the non-woven fabric before and after coating of the GNPs/sodium alginate solution were investigated. The thermal decomposition temperature of the fabric was increased from 230 °C to 240 °C, whereas the tensile stress increased from 99 MPa to 135 MPa. This suggested the enhancement quality offered by graphene as indicated in a lot of studies. Through temperature sensing tests, the developed sensor revealed a negative temperature coefficient feature with a TCR of $-1.55\%/^{\circ}\text{C}$ within 20–45 °C temperature range (Fig. 9(c)). The sensor also exhibited temperature distinguishability of 0.1 °C (inset of (Fig. 9(c))), stability over time (Fig. 9(d)), and repeatability (Fig. 9(d)), all

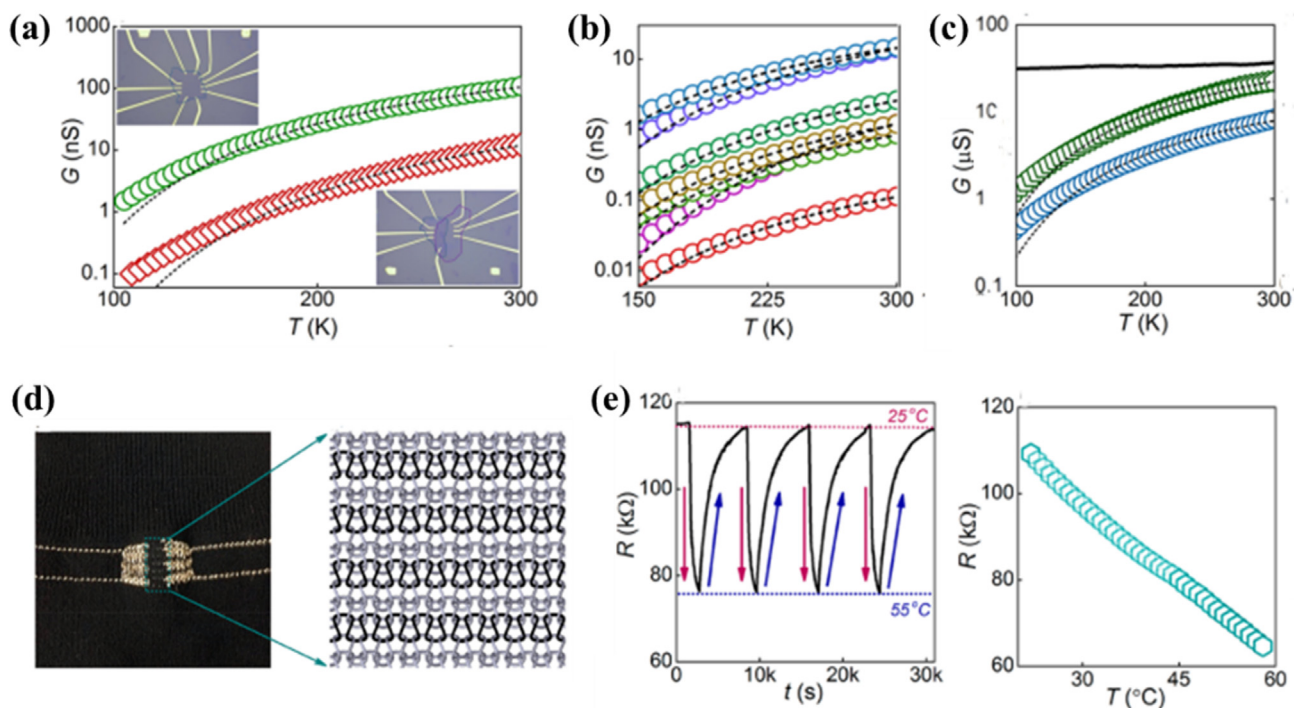


Fig. 7. Measured temperature-dependent conductance of fabricated sensors in [123]: (a) Si/SiO₂-supported single-rGO flakes (green) and double-layer overlapping (red) rGO flakes (the insets show microscopic images of each sample, respectively), (b) Si/SiO₂-supported drop-casted rGO with polymer/material ratio of ink droplets of 1:5 (top three lines) and 1:10 (bottom four lines), (c) graphene yarns coated with rGO (SH) (green), rGO (AA) (blue), and graphene flakes (black). Note: black dashed lines in (a)–(c) correspond to the exponential fittings. (d) Fabricated knitted temperature sensor using the developed rGO-coated yarns. For a better sensor performance, the graphene yarns were assembled only on the front side of the tubular knitted courses. (e) Resistance response of the knitted temperature sensor. Reproduced from [123] under a Creative Commons Attribution 4.0 International License (CC BY 4.0). Copyright (2019) American Chemical Society.

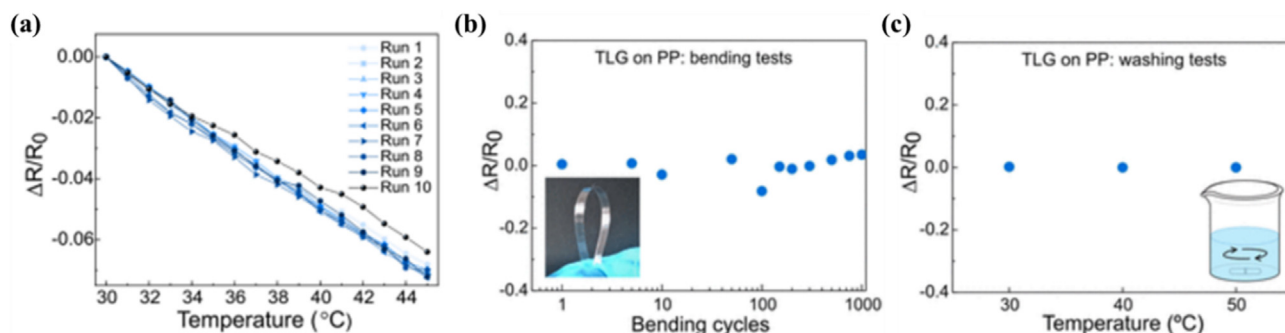


Fig. 8. (a) Temperature-dependent relative resistance change of TLG-based sensor developed in [67] for multiple temperature cycles. (b) Relative resistance change as a function of 5-mm radius bending cycles as shown in the inset. (c) Relative resistance change as a function of water temperature used in the washing test (60 min at 1000 rpm) illustrated in the inset. Reproduced from [67] under a Creative Commons Attribution 4.0 International License (CC BY 4.0). Copyright (2020) American Chemical Society.

of which demonstrated its applicability for wearable body temperature monitoring. Humidity seemed to affect slightly the performance of the sensor, showing an increased resistance with a maximum rate of 1.36% when the humidity increased from 20% to 100%. This was discovered to be the result of the balance between ionic conduction and swelling effects following the sensor exposure to moisture. At high humidity, hydronium ions (H₃O⁺) were produced as charge carries through the ionization of adsorbed water molecules. The transfer of these protons through ionic conductivity reduced sensor resistance. When water molecules entered into the sensor, however, the calcium alginate non-woven fabric swelled, resulting in an increase in graphene distance, hence, deterioration of graphene connectivity. This led to a decrease in sensor conductivity.

2.7. Graphene paper-based temperature sensors

Materials resembling free-standing paper or foil are an integral part of our technological society. Their uses have varied from printing, cleaning, packaging, toweling, to adhesive, electronic or optoelectronic components, batteries, supercapacitors, and molecular storage. The promising characteristics of graphene macroscopic architectures with hierarchical structures and the demand for graphene on a large scale, have led the researchers to develop graphene paper. Graphene paper is a highly organized structure, which uses graphene sheets as its building blocks. Due to the inherent planar structure of the graphene sheets, it is possible to effectively manage the periodic alignment of graphene nanosheets into 2D graphene papers through various non-covalent forces such

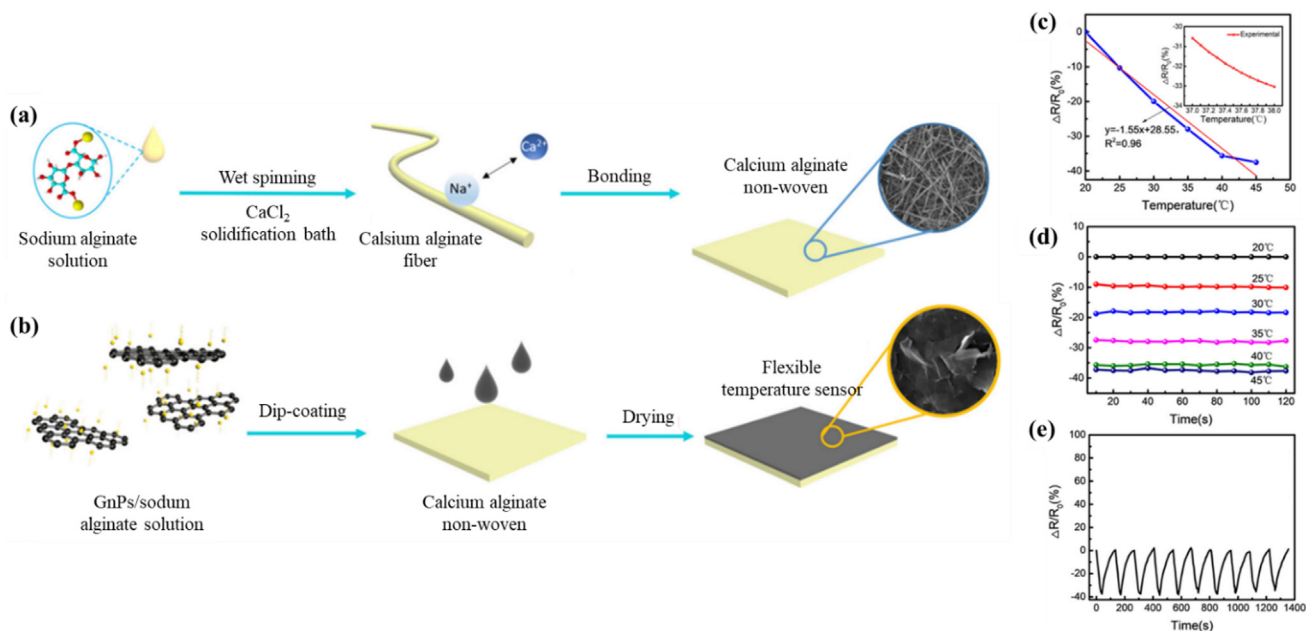


Fig. 9. Schematic illustrations of fabrication steps involved in [124]: (a) non-woven fabric fabrication through wet spinning and (b) sensor development through dip-coating. (c) Relative resistance change of the sensor as a function of temperature. (d) Temperature-dependent relative resistance change as a function of time. (e) Relative resistance change under repetitive cycles of heating up and cooling down in the temperature range of 20–45 °C. Reproduced from [124] with permission. Copyright (2019) Springer Nature B.V.

as hydrophobic effect, ionic interaction, hydrogen bonding and/or π - π stacking [125]. Recently, graphene papers have garnered a great deal of attention because of their low-cost, ease of production, versatile functionality, and most importantly their layer-by-layer hierarchical structures, which combine intralayer strong sp^2 bonds and interlayer crosslinks for efficient load transfer. Graphene papers can be prepared through phase assembly, electrochemical deposition, and CVD techniques, and subsequently functionalized with metal, metal oxide, polymer, semiconductor, or even enzymes and proteins to enable various desirable functions. Graphene composite materials in the form of paper are becoming more prevalent and are demonstrating their suitability for a variety of applications in the domains of energy storage, water purification, and sensing.

Gong et al. in [126] introduced the use of graphene paper for developing disposable temperature sensors. Such sensors are ben-

eficial in infectious disease control and public health security. Their complex manufacturing processes and poor performances, however, challenge their practical applications. The proposed concept in [126], on the other hand, allowed for relatively easy and low-cost fabrication of a flexible disposable sensor with high sensitivity. The sensor was developed by direct writing or mask spraying of graphene nanoribbons (GNRs) ink onto a common paper substrate. GNRs as a quasi-one-dimensional derivative of graphene offered interesting features that were advantageous for the development of disposable sensors. They included a good solution processability and a low defect density. The latter enabled GNRs to preserve good conductivity, allowing the prepared sensors to work directly without subsequent reduction process. Fig. 10(a) shows the schematic diagram of the fabrication process. The MWCNT was suspended in a potent oxidizer and catalytic agent (such as H_2SO_4 and $KMnO_4$) to allow MWCNT to split and expand to pro-

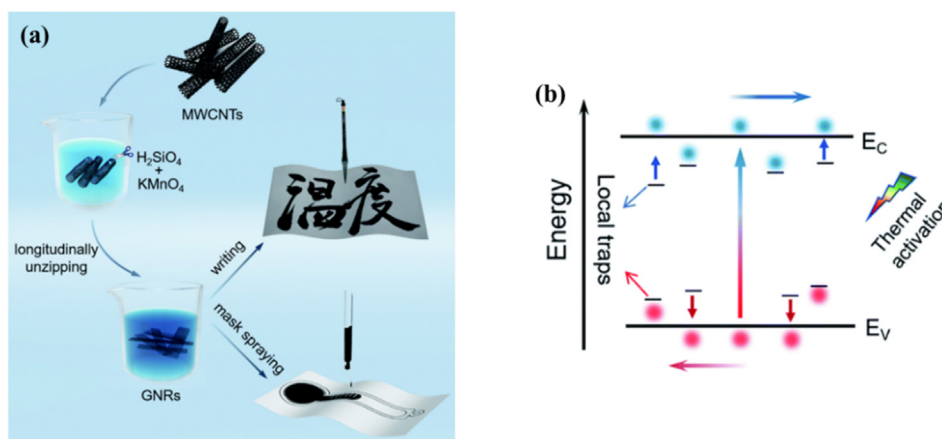


Fig. 10. (a) Schematic diagram of the fabrication process of GNRs-based temperature sensors in [126]. (b) Schematic diagram of thermal-activated carriers transport mechanism in the developed sensor. Reproduced from [126] under a Creative Commons Attribution-Non Commercial 3.0 Unported (CC BY-NC 3.0). Copyright (2020) The Authors.

duce nanoribbons. This process created the GNRs ink. In order to introduce certain oxygen-containing groups (such as hydroxyl and carboxyl) into the nanoribbons, the GNRs ink was further taken through an unzipping procedure. The induced oxygen-containing groups provided the ink improved stability and dispersity in polar solvent like water. The ink spraying process was completed using a PET-based plastic mask and a pair of metal masks. The final step included drying the prototypes at room temperature and encapsulating them with scotch tapes. Through measurements from 30°C to 80°C, the sensor showed a TCR of $-1.27\%/K$, showing a higher performance than most metals, which are in between 0.1 and $1\%/K$ [126]. The oxygen functional groups and nanoscale lateral dimensions provided GNRs with a certain bandgap and local traps in the energy band, hence enhancing the thermally-activated carrier transport. As illustrated in Fig. 10(b), by thermal activation, some carriers localized in the traps in the energy band can be released into the extend band, together with free carriers from intrinsic excitation. This resulted in the high temperature sensitivity of the developed sensor. Other advantages of the developed sensor included fast response and recovery time of 0.5 s, high resolution of up to 0.2 °C, and excellent bendable properties. The temperature sensor was also capable of performing other physiological parameters monitoring, including respiration rate and human touch.

3. Comparison of key performance

There are common attributes through which the performance of a graphene-based temperature sensor can be determined. They include stability, operating ranges, response/recovery time, and TCR. Among those, TCR is considered the most critical parameter as it represents the resistive nature of a component as a function of temperature. Higher values of TCR correspond to higher sensitivity. The value of TCR determines whether a component can be used in temperature sensing applications or simply as a stable resistor in highly reliable circuits and systems. For the prior case, a high TCR is expected, whereas a very low TCR is desired for the latter case. A positive TCR indicates an increase in resistance as temperature increases, whereas a negative TCR indicates a decrease in resistance as temperature increases. As seen in previous section, some graphene-based temperature sensors published in the literature displayed negative TCR values, whereas others exhibited positive TCR values. This interesting phenomenon may be related to the unique properties of graphene as a semi-metal and zero-bandgap semiconductor. When graphene has metallic characteristics, charge carriers scattering determines the temperature dependence of graphene resistance. As the temperature increases, the possibil-

ity of phonon/charge carriers scattering increases and mean free path of charge carriers reduces, which result in a decrease in charge carrier mobility and hence an increase in resistance [115]. On the other hand, when graphene shows semiconducting characteristics, thermally-activated charge carriers control the dependency of graphene resistance on temperature. As the temperature rises, the charge carriers mobility increases; hence, the resistance decreases [108]. Cheianov et. al. also postulated that a negative TCR in graphene is indicative of structural defects/disorders [105]. Table 1 compares the performance of some graphene-based temperature sensors reported in literature. We have also included Table 2, which lists some non-graphene-based sensors along with their corresponding performance. The two tables provide insight into the qualities that graphene may offer in the development of temperature sensors for wearable applications. It is seen that although the sensors presented in both the tables have been able to perform with high efficiency, the graphene-based sensors have additional interesting characteristics such as biocompatibility and transparency. The biocompatible nature is advantageous for wearable sensing as their ubiquitous presence would not create any irritation on the skin. The transparency of these sensors can be utilized to integrate with other flexible signal-conditioning circuits to form the next-generation transparent electronics. The response time of some graphene-based sensors is also comparatively faster than the non-graphene ones. This could be associated to the excellent electrical conductivity due to their zero band gap and high electron mobility. The transparency and response time of these graphene-based sensors can be varied by injecting other conducting and semiconducting nanomaterials. It is also seen through both tables that, the sensors whose composing materials have characteristics similar to graphene, exhibit qualities similar to graphene-based sensors. For example, the prototypes formed using CNTs show high flexibility, high operating range and TCR values in a similar range. It can also be inferred that the combination of any biocompatible polymer with these CNTs or other carbon-based allotrope would allow the sensors to be used for wearable applications.

The implementation of specific substrates and nanomaterials in each of these sensors simultaneously changes their characteristics, which allow them to be exploited for different applications. For example, the sensors having a wide linear range are ideal for industrial applications. Some of the specific uses under this category include processing of food and beverages, petrochemicals, cosmetics, pharmaceuticals and other engineering processes. Some of the substrates provide unique qualities supporting the fast response and high sensitivity of the developed sensors. For instance, the use of PI would increase the heat resistance, inherent fire-retardance and tear resistance. These sensors, when deployed as

Table 1
Performance Comparison of Different Graphene-based Temperature Sensors.

Ref	Materials	Operating range	TCR	Response time	Remark
[67]	Graphene, PP textiles	30–70 °C	$-0.17\%/^{\circ}C$	NA	Transparent, flexible, washable, durable
[75]	GNWs, PDMS	35–45 °C	$21.4\%/^{\circ}C$	~ 1.6 s	Flexible, stretchable, biocompatible
[76]	PHB/rGO, PET, PDMS	20–70 °C	$-0.8\%/^{\circ}C$	NA	Flexible, stretchable, water resistant, no hysteresis, sensor array
[103]	SA nanofibril/GO/PAM	25–65 °C	$-2\%/^{\circ}C$	~ 2.5 s	Flexible, stretchable, durable, multi modal sensing (strain, temperature)
[106]	GO, Al, Cu, Glass	$-40-0$ °C	59.3 kHz/ $^{\circ}C$	NA	-
		$10-60$ °C	46.1 kHz/ $^{\circ}C$		
[108]	rGO, PET, tape	30–100 °C	$-0.63\%/^{\circ}C$	~ 1.2 s	Flexible, durable, water resistant
[109]	rGO, PI, Cu	35–45 °C	$-0.743\%/^{\circ}C$	NA	Flexible, biocompatible
[112]	rGO, Pt	240–400 K	$-0.38\%/K$	NA	-
[113]	PEDOT:PSS/rGO/PDMS	30–50 °C	$-1.69\%/^{\circ}C$	NA	Flexible, stretchable, multi modal sensing (strain, temperature)
[115]	GNPs/PDMS	25–75 °C	$0.8\%/^{\circ}C$	$\sim 1.32-3.91$ s	Flexible, stretchable, durable, anti-interference (strain)
[121]	LIG, PI	20–60 °C	$-0.1\%/^{\circ}C$	NA	Flexible, easy & cost-effective manufacturing
[123]	LIG, PI	30–40 °C	$-0.041\%/^{\circ}C$	NA	Flexible, easy & cost-effective manufacturing
[124]	GNPs, Non-woven fabric	20–45 °C	$-1.55\%/^{\circ}C$	~ 26.3 s	Flexible, anti-interference (strain, humidity)
[126]	GNRs, paper	30–80 °C	$-1.27\%/K$	~ 0.5 s	Flexible, disposable, durable, sensor array

Table 2
Performance comparison of non-graphene-based temperature sensors.

Ref	Materials	Operating range	TCR	Response time	Remark
[20]	Ag, Kapton	20–60 °C	0.22%/°C	NA	Flexible, <5% hysteresis, simple fabrication
[130]	CNT, PEDOT:PSS	20–80 °C	–0.25%/°C	~1–2 s	Flexible, sensor array, multi modal sensing (strain-temperature)
[131]	Stainless-steel foil, aluminum nitride, gold, chromium	30–80 °C	–0.15%/°C	~1.7–2.3 s	Flexible
[132]	Ag, PEDOT:PSS, glossy paper	25–45 °C	0.094%/°C and –1.39%/°C	NA	Flexible, durable, multi modal sensing (temperature, strain, humidity), major hysteresis, disposable
[133]	Nickel, PI	–60–180 °C	0.44%/C	<10 s	Flexible, durable
[134]	MWCNTs/alumina composite	30–100 °C	–0.96%/°C	~40 s	Flexible, free standing film, 0.64% hysteresis
[135]	SWCNT TFTs, polyaniline nanofibers, PET	15–45 °C	–1%/°C	~1.8 s	Flexible, stretchable, durable, no hysteresis, sensor array
[136]	V ₂ O ₅	46–70 °C	–3%/°C to –4%/°C	NA	–
[137]	Ag, TPU	25–42 °C	0.234%/°C	NA	Flexible, 5.82% hysteresis
[138]	MWCNTs, Si	22–200 °C	0.103%/°C	NA	–

resistance temperature detectors (RTDs), can be used for electrical power generation, monitoring and controlling of furnaces, oil level sensors, intake air temperature sensors and automotive sensors in industries. The sensors having high TCR values are suitable for the measurement of the temperature of solids, liquids and gases in the domestic environment. The use of nanomaterials like metallic nanowires is not suggested in these kinds of sensors to minimize the toxicity levels. Certain graphene-based temperature sensors can also be used in different home appliances like refrigerators, air confectioners, heaters and freezers to maintain regular temperature for cooking and storage purposes. The use of some of these temperature sensors for wearable sensing would be beneficial if they are considered for both on-body and implantable sensing uses. The changes in the internal and external body temperature can be determined to study the effect of a medicine. These sensors can be attached to athletes can to monitor the minor changes in the core temperature. Apart from PDMS, other biocompatible polymers like polylactic acid [127], cellulose [128] and chitosan [129] should be used alongside graphene to form the wearable sensors. Nanoparticles with a size of <100 nm can be used to amalgamate with graphene to form composites-based temperature sensors.

4. Wireless sensor network

Wireless sensor network (WSN) is the key technology for continuous sensing and wirelessly transmitting data from the devel-

oped sensors described in the previous sections, particularly to enable the internet of things (IoT). Fig. 11 depicts a schematic diagram of typical wireless sensor network and the flow of the data from the sensing to the cloud [139]. Typically, sensors provide the data output in a digital or analogue form. If the sensor's capacitance or resistance changes as a function of the sensing parameter, a Capacitance to Digital Converter (CDC) or Resistance to Digital Convert (RDC) is typically required to convert the data into a digital form. In most cases, the sensor and signal conditioning circuit such as CDC and RDC have limited or no computation and processing capabilities, and thus an additional processing unit such as microcontroller unit (MCU) is incorporated for data processing. The processed data is subsequently transmitted wirelessly to the sink node or gateway/base station with the help of radio transceiver. Further, sink node or gateway forwards these data to the cloud via Wi-Fi, Ethernet or cellular network (e.g., 2G to 5G).

In the context of wearable healthcare sensors and systems, continuous accessibility and operation of the sensed data are generally required. The advancement of cloud computing technology provides a great opportunity to further analyze or store sensor data within the IoT cloud, where an authorized user may easily retrieve the data from any internet-connected device such as smart phone or computer as needed. Different technologies can be employed to enable wireless transmission, such as Bluetooth Low Energy (BLE), Radio Frequency Identification (RFID), Near Field Communication (NFC), ZigBee, and Long Range Wide Area Network (LoRaWAN) to name a few. The sensing device cost, the number of sensor nodes,

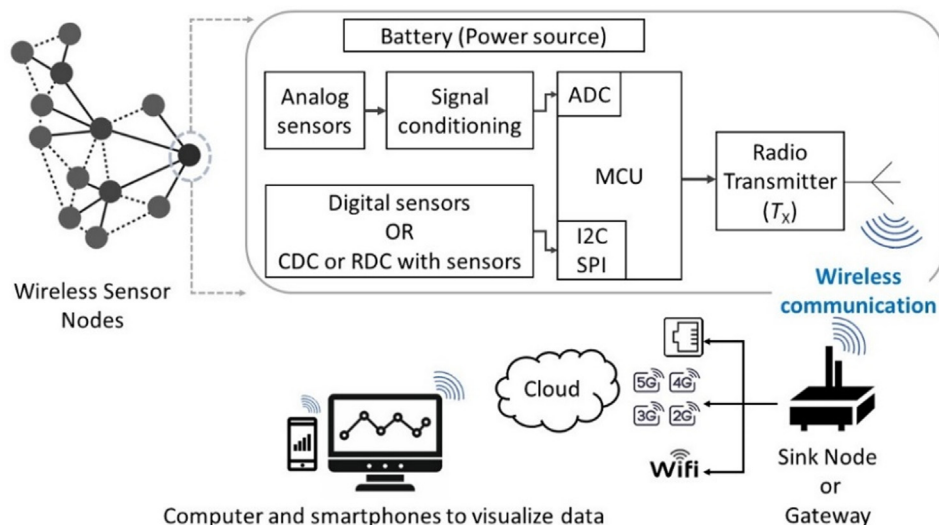


Fig. 11. Block diagram of a typical wireless sensor network.

the target communication range, the device life-time, and the power consumption are some major factors to consider when choosing a communication architecture. In regards to power, the consumption of the graphene-based temperature sensors is low, generally ranging from a few tens to a few hundreds of μW [67,100,140–142].

In [143], Kovalska et al. showed the use of battery as a power source to power the planar graphene-based temperature sensors. Sensed temperature was calculated from obtained sensor resistance value which was subsequently sent wirelessly to the data receiving unit. An experimental testbed based on WaspMote by Libelium evaluation board was designed for temperature measurement tests. WaspMote transferred the data through BLE to the user's smartphone, which then sent the received data to the ThingSpeak cloud service through Wi-Fi. The same practice was done by Somov et al. in [144]. The communication module was employed on a sensor tag board consisting of a microcontroller unit for processing the data and RF transmitter. The unit also consisted of an exponential filter to reduce the noise levels. The sensor tag transmitted the data to a smartphone using Bluetooth, which then sent the data to the cloud using Wi-Fi services. The wireless data transmission quality was tested in a direct line-of-sight condition from 0.5 to 10 m distance, where reasonable Received Signal Strength Indicator (RSSI) metrics were demonstrated, i.e., from 0.5 m (–59 dBm) to 10 m (–95 dBm).

Another work that incorporated wireless functionality for the transmission of monitored data can be seen in [145]. These devices measured the core body temperature by using graphene-inked infrared thermopile sensors. The sensors operated as ear-based devices fabricated using 3D printing technology. The communication system consisted of a data processing (Arduino Pro Mini) and a Bluetooth module. The entire sensing system operated on a 3.7 V, 850 mAh rechargeable lithium-polymer battery. The sensors were used for measuring the change in temperature of ten subjects under resting and exercising conditions for a total duration of 25 min. The graphene-inked thermopiles measured a temperature of 0.06 °C higher than that of the original MLX90614-DCA thermopile. The exercise caused an increase in the blood flow, causing an increase in the skin and skeletal muscles, and as a result of which, the heat was dissipated, leading to a small reduction of core temperature. Another example is shown in work done by Zhou et al. on flexible rGO-based temperature sensors integrated at a 3D-printed robot fingertip [146]. The robot finger was also used to house the integrated circuit having an external Bluetooth to allow for real-time sensing and wireless transmission of the sensed data to a mobile phone.

5. Challenges and opportunities

Although a significant amount of research has been conducted on the use of graphene in the fabrication of wearable temperature sensors, there are still gaps in the current sensors that need to be addressed.

When the precursor materials consisting of graphene platelets and graphene nanowalls are annealed to generate rGO, the heating temperature must be low and accurate [147,148] from a manufacturing standpoint. Otherwise, the mechanical strength of the generated rGO is severely compromised, affecting the overall performance of the sensors. Instead of nanocomposite-based sensors, the use of suspended graphene for producing flexible thermistors should be promoted. This is not only due to advantages such as high elasticity, optical transparency, high electron mobility, and high thermal and electrical conductivity [149], but also due to disadvantages associated with nanocomposite-based sensors, such as

compromised electrical conductivity, lack of structural integrity, long-term stability, and low repeatability of responses [150,151].

Alternatives to the CVD or Hummers method for the fabrication of graphene should be studied due to the high fabrication cost and generation of toxic gaseous by-products [152]. One alternative solution is laser-induced graphene, which is advantageous because to its eco-friendliness, adaptability, and adjustable morphologies [45]. In this regard, research should be encouraged into the possibility of photothermal graphene production from commercial polymers other than PI. A comparative analysis of the physicochemical properties of graphene products derived from different commercial polymers is required to reveal their sensing applications.

The cost of these sensors is an additional problem that must be addressed, particularly those requiring the use of standard photolithographic and etching processes. Employing additive techniques such as screen printing, inkjet printing, and 3D printing should be encouraged due to their low cost, high accuracy, speed, and capability to enable roll-to-roll production. Particularly, 3D printing technology enables the production of integrated and miniaturized sensor systems in a single manufacturing step. Further efforts are required not only on the development of graphene-based inks or 3D-printable filaments with rheological properties suited for an effective and efficient additive process, but also on the optimization of the printing process using the produced constituent materials. For instance, while using the 2D-printing techniques to fabricate the sensors, certain parameters like surface tension and viscosity of the inks on the flexible substrates should be analyzed and optimized to avoid the formation of an additive layers between the electrodes and substrates. Further thoughts on the sensor designs are required following the capabilities of the 2D or 3D printer technologies used. The formation of symmetrical electrode design, for example, should be encouraged for an efficient roll-to-roll 2D production. 3D printing, on the other hand, eliminates the manufacturing limitations that 2D printing imposes – practically any shape, complexity, and functionality can be realized. Various carbon or metallic nanomaterials can be incorporated within the conductive inks or printable filaments to boost certain qualities leading to a new generation of graphene-based temperature sensors.

The emergence of wearable electronics over the last decade has sparked a rising interest in clothing-integrated sensors as we enter the era of intelligent fabrics and even intelligent skin [104,153–161]. From just managing body temperature, other additional uses have evolved, including the ability to telecommunicate with humans or computers, detect changes in heart rhythm, track human activity, and even recreate the composition of human skin to aid healing. The fundamental mechanism behind these technologies is the employment of sensors that can detect a variety of parameters. In this context, the concept of enabling graphene-based temperature sensors with multifunctionality, including heating, sensing of humidity, strain, gas, blood pressure, and even biochemical, to name a few [18,62,155,162–164], while concurrently suitable for textile or skin integration, i.e. being flexible, elastic, breathable, and washable, must be advanced. The same thing applies to the concept of sensor array for improved sensitivity and selectivity. As a result of the COVID-19 health issue, it has become evident that creative ways to avoid infection are also required for smart textiles. From an application standpoint, adding antimicrobial capabilities to graphene textile-based sensors is an attractive path to study. In addition to protecting us from dangerous infections, another study area would be the development of intelligent sensors that do not pose a risk of provoking adverse immune reactions, therefore accelerating the healing process when applied to the skin. Using graphene-based sensors for detecting the variation of temperature during the administration of drugs or medicines would be an intriguing object of investigation in the

application domain. This will assist not only people in maintaining a balanced health state, but also the pharmaceutical industry in understanding the adjoining effects of newly created medications. The change in human body temperature in relation to an individual's emotional state may also be examined to aid businesses in identifying the anxiety level associated with each assignment. The link of these graphene-based temperature sensors to the food industry is also possible, since the influence of each ingestible item on the body's temperature over time may assist in determining the appropriate diet for individuals.

Further work should also be done on the aspect of sensitivity, robustness and longevity of graphene-based temperature sensors. The modification of the graphene band gap in order to tailor the sensitivity of prototypes is one of the areas that may be further explored. Mixing semiconducting nanoparticles may also be used to improve accuracy and precision while simultaneously reducing power consumption. Selecting nanomaterials with a low Young's modulus will boost the mechanical flexibility of the sensors. Graphene should be combined with hydrophobic materials in order to maximize the washability of the resulting sensors. Further investigations are required to boost further the robustness of graphene-based sensors against multiple washing. Other polymers than PDMS should be used to build the substrates of these sensors in order to achieve water resistance and biocompatibility. Additionally, the toxicity of body-attached sensors should be investigated further. In the context of flexible, stretchable, and bendable temperature sensors, it is, however, challenging to balance between having high temperature sensitivity and high flexibility/stretchability. In the literature, often highly-sensitive sensors are limited to low strain ranges. On the other hand, to ensure sensing accuracy in wearable applications, often the temperature sensitivity should also be independent of the strain applied to the sensors. There are still spaces for further investigations of graphene to the above context.

6. Conclusions

This article provides a comprehensive overview of the development and implementation of wearable temperature sensors based on graphene. The significance of temperature measurement lies in the ability to study the condition of a subject under the influence of different environmental conditions. Graphene has been used in a variety of forms as a sensing element, with its physiochemical compositions influencing the performance of the resulting sensing device. Diverse manufacturing strategies were described for fabricating temperature sensors using various graphene variants in conjunction with other materials. Sensor characterizations were conducted as a proof-of-concept and in real time scenario across a wide temperature range. In order to monitor sensed data, the developed devices performed through wired and wireless operations. The graphene sensors were combined with a communication module, such as BLE, to transmit data to the monitoring unit for further analysis. Graphene-based wearable sensors have a significant potential for multifunctional applications that may be investigated to expand the influence of nanomaterials-based sensing systems on people and society. Significant progress has been achieved, yet much remains to be accomplished.

Declaration of Competing Interest

The authors declare that they have no known competing financial interests or personal relationships that could have appeared to influence the work reported in this paper.

Acknowledgement

The project is supported in part by the German Research Foundation (DFG, Deutsche Forschungsgemeinschaft) as part of Germany's Excellence Strategy – EXC 2050/1 – Project ID 390696704 – Cluster of Excellence “Centre for Tactile Internet with Human-in-the-Loop” (CeTI) of Technische Universität Dresden, in part by the Enterprise Ireland funded HOLISTICS DTIF project (EIDT20180291-A), in part by Science Foundation Ireland (SFI) under the following Grant Numbers: the SFI Centre VistaMilk (SFI 16/RC/3835), the Connect Centre for Future Networks and Communications (13/RC/2077) and the Insight Centre for Data Analytics (SFI/12/RC/2289), as well as by the European Regional Development Fund.

References

- [1] R. Jaaniso, O.K. Tan, *Semiconductor Gas Sensors*, Elsevier, 2013.
- [2] S.M. Sze, *Semiconductor Sensors*, John Wiley & Sons, 1994.
- [3] M.F. Frasco, N. Chaniotakis, Semiconductor quantum dots in chemical sensors and biosensors, *Sensors* 9 (9) (2009) 7266–7286.
- [4] X. Yongqing, Y. Yongjun, Processing technology and development of silicon MEMS, *Micronanoelectron. Technol.* 147 (2010) 425–431.
- [5] C. Hindrichsen, R. Lou-Møller, K. Hansen, E.V. Thomsen, Advantages of PZT thick film for MEMS sensors, *Sens. Actuat., A* 163 (1) (2010) 9–14.
- [6] J.W. Judy, Microelectromechanical systems (MEMS): fabrication, design and applications, *Smart Mater. Struct.* 10 (6) (2001) 1115.
- [7] A. Nag, A.I. Zia, X. Li, S.C. Mukhopadhyay, J. Kosel, Novel sensing approach for LPG leakage detection: Part I—Operating mechanism and preliminary results, *IEEE Sens. J.* 16 (4) (2015) 996–1003.
- [8] M.E.E. Alahi, L. Xie, S. Mukhopadhyay, L. Burkitt, A temperature compensated smart nitrate-sensor for agricultural industry, *IEEE Trans. Ind. Electron.* 64 (9) (2017) 7333–7341.
- [9] Y. Zhao, L. Zhao, Z. Jiang, High temperature and frequency pressure sensor based on silicon-on-insulator layers, *Meas. Sci. Technol.* 17 (3) (2006) 519.
- [10] N. Afsarimanesh, A. Nag, M.E.E. Alahi, T. Han, S.C. Mukhopadhyay, Interdigital sensors: biomedical, environmental and industrial applications, *Sens. Actuat. A: Phys.* (2020) 111923.
- [11] Y. Xu et al., Silicon-based sensors for biomedical applications: a review, *Sensors* 19 (13) (2019) 2908.
- [12] N. Afsarimanesh, M.E.E. Alahi, S.C. Mukhopadhyay, M. Kruger, Development of IoT-based impedometric biosensor for point-of-care monitoring of bone loss, *IEEE J. Emerg. Sel. Top. Circ. Syst.* 8 (2) (2018) 211–220.
- [13] A. Nag et al., A transparent strain sensor based on PDMS-embedded conductive fabric for wearable sensing applications, *IEEE Access* 6 (2018) 71020–71027.
- [14] A. Nag, S.C. Mukhopadhyay, J. Kosel, Wearable flexible sensors: a review, *IEEE Sens. J.* 17 (13) (2017) 3949–3960.
- [15] H. Liu et al., Electrically conductive polymer composites for smart flexible strain sensors: a critical review, *J. Mater. Chem. C* 6 (45) (2018) 12121–12141.
- [16] Y. Xiao, S. Jiang, Y. Li, W. Zhang, Screen-printed flexible negative temperature coefficient temperature sensor based on polyvinyl chloride/carbon black composites, *Smart Mater. Struct.* 30 (2) (2021) 025035.
- [17] S. Yoon, H.-K. Kim, Cost-effective stretchable Ag nanoparticles electrodes fabrication by screen printing for wearable strain sensors, *Surf. Coat. Technol.* 384 (2020) 125308.
- [18] Y. Poo-arporn, S. Pakapongpan, N. Chanlek, R.P. Poo-arporn, The development of disposable electrochemical sensor based on Fe3O4-doped reduced graphene oxide modified magnetic screen-printed electrode for ractopamine determination in pork sample, *Sens. Actuat., B* 284 (2019) 164–171.
- [19] D.D. Le, T.N.N. Nguyen, D.C.T. Doan, T.M.D. Dang, M.C. Dang, Fabrication of interdigitated electrodes by inkjet printing technology for application in ammonia sensing, *Adv. Nat. Sci.: Nanosci. Nanotechnol.* 7 (2) (2016) 025002.
- [20] M. Dankoco, G. Tesfay, E. Bènevent, M. Bendahan, Temperature sensor realized by inkjet printing process on flexible substrate, *Mater. Sci. Eng., B* 205 (2016) 1–5.
- [21] A. Moya, G. Gabriel, R. Villa, F.J. del Campo, Inkjet-printed electrochemical sensors, *Curr. Opin. Electrochem.* 3 (1) (2017) 29–39.
- [22] F. Stan, N.-V. Stanciu, A.-M. Constantinescu, C. Fetecau, 3D printing of flexible and stretchable parts using multiwall carbon nanotube/polyester-based thermoplastic polyurethane, *J. Manuf. Sci. Eng.* (2020) 1–33.
- [23] T. Xiao, C. Qian, R. Yin, K. Wang, Y. Gao, F. Xuan, 3D printing of flexible strain sensor array based on UV-curable multiwalled carbon nanotube/elastomer composite, *Adv. Mater. Technol.* (2020) 2000745.
- [24] S. He, S. Feng, A. Nag, N. Afsarimanesh, T. Han, S.C. Mukhopadhyay, Recent progress in 3D printed mold-based sensors, *Sensors* 20 (3) (2020) 703.
- [25] A. Nag, S.C. Mukhopadhyay, J. Kosel, Sensing system for salinity testing using laser-induced graphene sensors, *Sens. Actuat., A* 264 (2017) 107–116.

- [26] E.A. Mwafy, A.M. Mostafa, Multi walled carbon nanotube decorated cadmium oxide nanoparticles via pulsed laser ablation in liquid media, *Opt. Laser Technol.* 111 (2019) 249–254.
- [27] A. Nag, S.C. Mukhopadhyay, J. Kosel, Flexible carbon nanotube nanocomposite sensor for multiple physiological parameter monitoring, *Sens. Actuat., A* 251 (2016) 148–155.
- [28] I. Akhtar, S.H. Chang, Stretchable sensor made of MWCNT/ZnO nanohybrid particles in PDMS, *Adv. Mater. Technol.* 5 (9) (2020) 2000229.
- [29] M. Parmeggiani et al., PDMS/polyimide composite as an elastomeric substrate for multifunctional laser-induced graphene electrodes, *ACS Appl. Mater. Interfaces* 11 (36) (2019) 33221–33230.
- [30] A. Nag, S.C. Mukhopadhyay, J. Kosel, Tactile sensing from laser-abeted metallized PET films, *IEEE Sens. J.* 17 (1) (2016) 7–13.
- [31] S. Li et al., The room temperature gas sensor based on Polyaniline@ flower-like WO₃ nanocomposites and flexible PET substrate for NH₃ detection, *Sens. Actuat., B* 259 (2018) 505–513.
- [32] U. Altenberend et al., Towards fully printed capacitive gas sensors on flexible PET substrates based on Ag interdigitated transducers with increased stability, *Sens. Actuat., B* 187 (2013) 280–287.
- [33] T. Han et al., Gold/polyimide-based resistive strain sensors, *Electronics* 8 (5) (2019) 565.
- [34] Y. Qin et al., Lightweight, superelastic, and mechanically flexible graphene/polyimide nanocomposite foam for strain sensor application, *ACS Nano* 9 (9) (2015) 8933–8941.
- [35] G. Márton, G. Orbán, M. Kiss, R. Fiáth, A. Pongrácz, I. Ulbert, A multimodal, SU-8-platinum-polyimide microelectrode array for chronic in vivo neurophysiology, *PLoS ONE* 10 (12) (2015) e0145307.
- [36] G. Shen et al., Transparent and stretchable strain sensors with improved microstructure, *Adv. Electron. Mater.* 6 (8) (2020) 1901360.
- [37] J. Ramírez, D. Rodríguez, A.D. Urbina, A.M. Cardenas, D.J. Lipomi, Combining high sensitivity and dynamic range: wearable thin-film composite strain sensors of graphene, ultrathin palladium, and PEDOT: PSS, *ACS Appl. Nano Mater.* 2 (4) (2019) 2222–2229.
- [38] Y. Seekaew, S. Lokavee, D. Phokharatkul, A. Wisitsoraat, T. Kerdcharoen, C. Wongchoosuk, Low-cost and flexible printed graphene-PEDOT: PSS gas sensor for ammonia detection, *Org. Electron.* 15 (11) (2014) 2971–2981.
- [39] Y. Yu, S. Peng, P. Blanloeuil, S. Wu, C.H. Wang, Wearable temperature sensors with enhanced sensitivity by engineering microcrack morphology in PEDOT: PSS-PDMS sensors, *ACS Appl. Mater. Interf.* 12 (32) (2020) 36578–36588, <https://doi.org/10.1021/acami.0c07649>.
- [40] T. Han, A. Nag, S.C. Mukhopadhyay, Y. Xu, Carbon nanotubes and its gas-sensing applications: a review, *Sens. Actuat. A* 291 (2019) 107–143.
- [41] H.-L. Kao, C.-L. Cho, L.-C. Chang, C.-B. Chen, W.-H. Chung, Y.-C. Tsai, A fully inkjet-printed strain sensor based on carbon nanotubes, *Coatings* 10 (8) (2020) 792.
- [42] R. Daňová, R. Olejník, P. Slobodian, J. Matyas, The piezoresistive highly elastic sensor based on carbon nanotubes for the detection of breath, *Polymers* 12 (3) (2020) 713.
- [43] A. Nag, A. Mitra, S.C. Mukhopadhyay, Graphene and its sensor-based applications: a review, *Sens. Actuat. A* 270 (2018) 177–194.
- [44] A. Mehmood et al., Graphene based nanomaterials for strain sensor application—a review, *J. Environ. Chem. Eng.* 8 (3) (2020) 103743.
- [45] L. Huang, J. Su, Y. Song, R. Ye, Laser-induced graphene: en route to smart sensing, *Nano-Micro Lett.* 12 (1) (2020) 1–17.
- [46] A.S. Kurian, V.B. Mohan, D. Bhattacharyya, Embedded large strain sensors with graphene-carbon black-silicone rubber composites, *Sens. Actuat. A* 282 (2018/10/15/2018,) 206–214, <https://doi.org/10.1016/j.sna.2018.09.017>.
- [47] A. Nag, S. Feng, S. Mukhopadhyay, J. Kosel, D. Inglis, 3D printed mould-based graphite/PDMS sensor for low-force applications, *Sens. Actuat., A* 280 (2018) 525–534.
- [48] A. Nag, N. Afasrimanesh, S. Feng, S.C. Mukhopadhyay, Strain induced graphite/PDMS sensors for biomedical applications, *Sens. Actuat., A* 271 (2018) 257–269.
- [49] S. Tadakaluru, W. Thongsuwan, P. Singjai, Stretchable and flexible high-strain sensors made using carbon nanotubes and graphite films on natural rubber, *Sensors* 14 (1) (2014) 868–876.
- [50] A.S. Kurian, V.B. Mohan, H. Souri, J. Leng, D. Bhattacharyya, Multifunctional flexible and stretchable graphite-silicone rubber composites, *J. Mater. Res. Technol.* 9 (6) (2020/11/01/2020,) 15621–15630, <https://doi.org/10.1016/j.jmrt.2020.11.021>.
- [51] Y. Peng, D. Lin, J.J. Gooding, Y. Xue, L. Dai, Flexible fiber-shaped nonenzymatic sensors with a graphene-metal heterostructure based on graphene fibres decorated with gold nanosheets, *Carbon* 136 (2018) 329–336.
- [52] N. Elahi, M. Kamali, M.H. Baghersad, Recent biomedical applications of gold nanoparticles: a review, *Talanta* 184 (2018) 537–556.
- [53] S. Gong et al., Tattolike polyaniline microparticle-doped gold nanowire patches as highly durable wearable sensors, *ACS Appl. Mater. Interf.* 7 (35) (2015) 19700–19708.
- [54] S. Jeong, S. Heo, M. Kang, H.-J. Kim, Mechanical durability enhancement of gold-nanosheet stretchable electrodes for wearable human bio-signal detection, *Mater. Des.* 196 (2020) 109178, <https://doi.org/10.1016/j.matdes.2020.109178>.
- [55] M. Maruthupandy, G. Rajivgandhi, T. Muneeswaran, T. Venilla, F. Quero, J.-M. Song, Chitosan/silver nanocomposites for colorimetric detection of glucose molecules, *Int. J. Biol. Macromol.* 121 (2019) 822–828.
- [56] W. Zhang, Q. Liu, P. Chen, Flexible strain sensor based on carbon black/silver nanoparticles composite for human motion detection, *Materials* 11 (10) (2018) 1836.
- [57] H. Lee, B. Seong, H. Moon, D. Byun, Directly printed stretchable strain sensor based on ring and diamond shaped silver nanowire electrodes, *RSC Adv.* 5 (36) (2015) 28379–28384.
- [58] X. Meng, J. Yang, Z. Liu, W. Lu, Y. Sun, Y. Dai, Non-contact, fibrous cellulose acetate/aluminum flexible electronic-sensor for humidity detecting, *Compos. Commun.* (2020).
- [59] L. Lamanna et al., Flexible and transparent aluminum-nitride-based surface-acoustic-wave device on polymeric polyethylene naphthalate, *Adv. Electron. Mater.* 5 (6) (2019) 1900095.
- [60] H.G. Yeo, J. Jung, M. Sim, J.E. Jang, H. Choi, Integrated piezoelectric aln thin film with SU-8/PDMS supporting layer for flexible sensor array, *Sensors* 20 (1) (2020) 315.
- [61] S. Zhang et al., A flexible bifunctional sensor based on porous copper nanowire@ IonGel composite films for high-resolution stress/deformation detection, *J. Mater. Chem. C* 8 (12) (2020) 4081–4092.
- [62] Y. Zhang et al., A flexible non-enzymatic glucose sensor based on copper nanoparticles anchored on laser-induced graphene, *Carbon* 156 (2020) 506–513.
- [63] S. Ammara, S. Shamaila, R. Sharif, S. Ghani, N. Zafar, Uniform and homogeneous growth of copper nanoparticles on electrophoretically deposited carbon nanotubes electrode for nonenzymatic glucose sensor, *Acta Metall. Sin. (English Lett.)* 29 (10) (2016) 889–894.
- [64] R. Sankar, X.H. Le, S. Lee, D. Wang, Protection of data confidentiality and patient privacy in medical sensor networks, in: *Implantable Sensor Systems for Medical Applications*, Elsevier, 2013, pp. 279–298.
- [65] H. Chen, M. Xue, Z. Mei, S. Bambang Oetomo, W. Chen, A review of wearable sensor systems for monitoring body movements of neonates, *Sensors* 16 (12) (2016) 2134.
- [66] S. Patel, H. Park, P. Bonato, L. Chan, M. Rodgers, A review of wearable sensors and systems with application in rehabilitation, *J. NeuroEng. Rehabil.* 9 (1) (2012) 1–17.
- [67] G. Rajan et al., Low operating voltage carbon-graphene hybrid e-textile for temperature sensing, *ACS Appl. Mater. Interf.* 12 (26) (2020) 29861–29867.
- [68] T.H. Kim, S.J. Kim, Development of a micro-thermal flow sensor with thin-film thermocouples, *J. Micromech. Microeng.* 16 (11) (2006) 2502–2508, <https://doi.org/10.1088/0960-1317/16/11/035>.
- [69] J.-J. Park, M. Taya, Design of micro-temperature sensor array with thin film thermocouples, *J. Electron. Packag.* 127 (3) (2004) 286–289, <https://doi.org/10.1115/1.1997157>.
- [70] Y. Moser, M.A.M. Gijs, Miniaturized flexible temperature sensor, *J. Microelectromech. Syst.* 16 (6) (2007) 1349–1354, <https://doi.org/10.1109/JMEMS.2007.908437>.
- [71] J. Jeon, H.-B.-R. Lee, Z. Bao, Flexible wireless temperature sensors based on ni microparticle-filled binary polymer composites, *Adv. Mater.* 25 (6) (2013) 850–855, <https://doi.org/10.1002/adma.201204082>.
- [72] T. Someya et al., Conformable, flexible, large-area networks of pressure and thermal sensors with organic transistor active matrixes, *Proc. Natl. Acad. Sci. U.S.A.* 102(35) (2005) 12321. doi: 10.1073/pnas.0502392102.
- [73] N.T. Tien et al., “A flexible bimodal sensor array for simultaneous sensing of pressure and temperature,” (in eng), *Adv. Mater.* 26 (5) (2014) 796–804, <https://doi.org/10.1002/adma.201302869>.
- [74] X. Ren, P.K.L. Chan, J. Lu, B. Huang, D.C.W. Leung, High dynamic range organic temperature sensor, *Adv. Mater.* 25 (9) (2013) 1291–1295, <https://doi.org/10.1002/adma.201204396>.
- [75] J. Yang et al., Wearable temperature sensor based on graphene nanowalls, *RSC Adv.* 5 (32) (2015) 25609–25615.
- [76] L. Dan, A.L. Elias, Flexible and stretchable temperature sensors fabricated using solution-processable conductive polymer composites, *Adv. Healthcare Mater.* 9 (16) (2020) 2000380.
- [77] L. Dan, A.L. Elias, Flexible and stretchable temperature sensors fabricated using solution-processable conductive polymer composites, *Adv. Healthcare Mater.* 9(16) (2020) 2000380. doi:10.1002/adhm.202000380.
- [78] A.K. Geim, K.S. Novoselov, “The rise of graphene,” in *Nanoscience and technology: a collection of reviews from nature journals*, World Scientific (2010) 11–19.
- [79] T. Xu, Z. Zhang, L. Qu, Graphene-based fibers: recent advances in preparation and application, *Adv. Mater.* 32 (5) (2020) 1901979.
- [80] K.S. Novoselov et al., Electric field effect in atomically thin carbon films, *Science* 306 (5696) (2004) 666, <https://doi.org/10.1126/science.1102896>.
- [81] A. Nag, M.E.E. Alahi, S.C. Mukhopadhyay, Recent progress in the fabrication of graphene fibers and their composites for applications of monitoring human activities, *Appl. Mater. Today* 22 (2021) 100953.
- [82] F. Wang, L. Liu, W.J. Li, Graphene-based glucose sensors: a brief review, *IEEE Trans. Nanobiosci.* 14(8) (2015) 818–834.
- [83] A.A. Balandin et al., Superior thermal conductivity of single-layer graphene, *Nano Lett.* 8 (3) (2008) 902–907, <https://doi.org/10.1021/nl0718372>.
- [84] B. Davaji et al., A patterned single layer graphene resistance temperature sensor, *Sci. Rep.* 7 (1) (2017) 1–10.
- [85] T.Q. Trung, N.T. Tien, D. Kim, J.H. Jung, O.J. Yoon, N.-E. Lee, High thermal responsiveness of a reduced graphene oxide field-effect transistor, *Adv. Mater.* 24 (38) (2012) 5254–5260, <https://doi.org/10.1002/adma.201201724>.
- [86] T.Q. Trung, S. Ramasundaram, S.W. Hong, N.-E. Lee, Flexible and transparent nanocomposite of reduced graphene oxide and P(VDF-TrFE) copolymer for

- high thermal responsivity in a field-effect transistor, *Adv. Funct. Mater.* 24 (22) (2014) 3438–3445, <https://doi.org/10.1002/adfm.201304224>.
- [87] W. Choi, I. Lahiri, R. Seelaboyina, Y.S. Kang, Synthesis of graphene and its applications: a review, *Crit. Rev. Solid State Mater. Sci.* 35 (1) (2010) 52–71, <https://doi.org/10.1080/10408430903505036>.
- [88] D.R. Cooper et al., Experimental review of graphene, *ISRN Condens. Matter Phys.* 2012 (2012) 501686, <https://doi.org/10.5402/2012/501686>.
- [89] A.H. Castro Neto, F. Guinea, N.M.R. Peres, K.S. Novoselov, A.K. Geim, The electronic properties of graphene, *Rev. Modern Phys.* 81(1) (2009) 109–162. doi: 10.1103/RevModPhys.81.109.
- [90] P. Avouris, Graphene: electronic and photonic properties and devices, *Nano Lett.* 10 (11) (2010) 4285–4294, <https://doi.org/10.1021/nl102824h>.
- [91] M.M. Islam, S.S. Ahmed, M. Rashid, M.M. Akanda, Mechanical and thermal properties of graphene over composite materials: a technical review, *J. Cast. Mater. Eng.* 3 (1) (2019) 19.
- [92] Y. Zhu et al., Graphene and graphene oxide: synthesis, properties, and applications, *Adv. Mater.* 22 (35) (2010) 3906–3924, <https://doi.org/10.1002/adma.201001068>.
- [93] Y. Shao, J. Wang, H. Wu, J. Liu, I.A. Aksay, Y. Lin, Graphene based electrochemical sensors and biosensors: a review, *Electroanal.: Int. J. Devot. Fund. Pract. Aspects Electroanal.* 22 (10) (2010) 1027–1036.
- [94] Y. Zhao, X.-G. Li, X. Zhou, Y.-N. Zhang, Review on the graphene based optical fiber chemical and biological sensors, *Sens. Actuat., B* 231 (2016) 324–340.
- [95] F. Wang, L. Liu, W.J. Li*, Graphene-based glucose sensors: a brief review, *IEEE Trans. NanoBiosci.* 14(8) (2015) 818–834. doi: 10.1109/TNB.2015.2475338.
- [96] T. Wang, Z. Ouyang, F. Wang, Y. Liu, A review on graphene strain sensors based on fiber assemblies, *SN Appl. Sci.* 2 (2020) 1–22.
- [97] J. Zhao, G.-Y. Zhang, D.-X. Shi, Review of graphene-based strain sensors, *Chin. Phys. B* 22 (5) (2013) 057701, <https://doi.org/10.1088/1674-1056/22/5/057701>.
- [98] T. Wang et al., A review on graphene-based gas/vapor sensors with unique properties and potential applications, *Nano-Micro Lett.* 8 (2) (2016) 95–119.
- [99] S. Gupta Chatterjee, S. Chatterjee, A.K. Ray, A.K. Chakraborty, Graphene–metal oxide nanohybrids for toxic gas sensor: a review, *Sens. Actuat., B* 221 (2015) 1170–1181, <https://doi.org/10.1016/j.snb.2015.07.070>.
- [100] H. Huang et al., Graphene-based sensors for human health monitoring, *Front. Chem.* 7 (2019) 399.
- [101] P.R. Wallace, The band theory of graphite, *Phys. Rev.* 71(9) (1947) 622–634. doi: 10.1103/PhysRev.71.622.
- [102] S. Stankovich et al., Synthesis of graphene-based nanosheets via chemical reduction of exfoliated graphite oxide, *Carbon* 45 (7) (2007) 1558–1565, <https://doi.org/10.1016/j.carbon.2007.02.034>.
- [103] W. Hou, Z. Luan, D. Xie, X. Zhang, T. Yu, K. Sui, High performance dual strain-temperature sensor based on alginate nanofibril/graphene oxide/polyacrylamide nanocomposite hydrogel, *Compos. Commun.* 100837 27 (2021), <https://doi.org/10.1016/j.coco.2021.100837>.
- [104] Q. Wang, S. Ling, X. Liang, H. Wang, H. Lu, Y. Zhang, Self-healable multifunctional electronic tattoos based on silk and graphene, *Adv. Funct. Mater.* 29 (16) (2019) 1808695, <https://doi.org/10.1002/adfm.201808695>.
- [105] V.V. Cheianov, V.I. Fal'ko, Friedel oscillations, impurity scattering, and temperature dependence of resistivity in graphene, (in eng), *Phys. Rev. Lett.* 97(22) (2006) 226801. doi: 10.1103/PhysRevLett.97.226801.
- [106] Q.-Y. Ren, J.-Q. Huang, L.-F. Wang, S. Wan, L.-T. Sun, Q.-A. Huang, Temperature sensing properties of the passive wireless sensor based on graphene oxide films, in: *SENSORS, 2014 IEEE, IEEE, 2014*, pp. 432–435.
- [107] R. Tarcan, O. Todor-Boer, I. Petrovai, C. Leordean, S. Astilean, I. Botiz, Reduced graphene oxide today, *J. Mater. Chem. C*, 8(4) (2020) 1198–1224. doi: 10.1039/C9TC04916A.
- [108] G. Liu et al., A flexible temperature sensor based on reduced graphene oxide for robot skin used in internet of things, *Sensors* 18 (5) (2018) 1400.
- [109] P. Sahatiya, S.K. Puttapati, V.V. Srikanth, S. Badhulika, Graphene-based wearable temperature sensor and infrared photodetector on a flexible polyimide substrate, *Flexible Printed Electron.* 1 (2) (2016) 025006.
- [110] J. T. W. Kuo, L. Yu, E. Meng, Micromachined thermal flow sensors—a review, *Micromachines* 3(3) (2012) 550–573. <<https://www.mdpi.com/2072-666X/3/3/550>>.
- [111] C. Gómez-Navarro et al., Electronic transport properties of individual chemically reduced graphene oxide sheets, *Nano Lett.* 7 (11) (2007) 3499–3503, <https://doi.org/10.1021/nl072090c>.
- [112] G. Khurana, S. Sahoo, S. Barik, N. Kumar, G. Sharma, Reduced graphene oxide as an ex-celent temperature sensor, *J. Nanosci. Nanotechnol.* 2 (2018) 101.
- [113] F. Zhang et al., Multi-modal strain and temperature sensor by hybridizing reduced graphene oxide and PEDOT:PSS, *Compos. Sci. Technol.* 187 (2020) 107959, <https://doi.org/10.1016/j.compscitech.2019.107959>.
- [114] P. Wick et al., Classification Framework for Graphene-Based Materials, *Angew. Chem. Int. Ed.* 53 (30) (2014) 7714–7718, <https://doi.org/10.1002/anie.201403335>.
- [115] Z. Wang et al., 3D-printed graphene/polydimethylsiloxane composites for stretchable and strain-insensitive temperature sensors, *ACS Appl. Mater. Interfaces* 11 (1) (2018) 1344–1352.
- [116] Z. Wang et al., An ultralight graphene honeycomb sandwich for stretchable light-emitting displays, *Adv. Funct. Mater.* 28 (19) (2018) 1707043, <https://doi.org/10.1002/adfm.201707043>.
- [117] C. Yang, H. Bi, D. Wan, F. Huang, X. Xie, M. Jiang, Direct PECVD growth of vertically erected graphene walls on dielectric substrates as excellent multifunctional electrodes, *J. Mater. Chem. A* 1(3) (2013) 770–775. doi: 10.1039/C2TA00234E.
- [118] X. Song et al., Direct versatile PECVD growth of graphene nanowalls on multiple substrates, *Mater. Lett.* 137 (2014) 25–28, <https://doi.org/10.1016/j.matlet.2014.08.125>.
- [119] N. Dixit, S.P. Singh, Laser-Induced Graphene (LIG) as a smart and sustainable material to restrain pandemics and endemics: a perspective, *ACS Omega* 7 (6) (2022) 5112–5130, <https://doi.org/10.1021/acsomega.1c06093>.
- [120] J. Liu et al., Laser-induced graphene (LIG)-driven medical sensors for health monitoring and diseases diagnosis, *Microchim. Acta* 189 (2) (2022) 54, <https://doi.org/10.1007/s00604-021-05157-6>.
- [121] M. Marengo, G. Marinaro, J. Kosel, Flexible temperature and flow sensor from laser-induced graphene, in: *2017 IEEE SENSORS, IEEE, 2017*, pp. 1–3.
- [122] H. Kun, L. Bin, M. Orban, Q. Donghai, Y. Hongbo, Accurate flexible temperature sensor based on laser-induced graphene material, *Shock Vib.* 2021 (2021) 9938010, <https://doi.org/10.1155/2021/9938010>.
- [123] S. Afroj et al., Engineering graphene flakes for wearable textile sensors via highly scalable and ultrafast yarn dyeing technique, *ACS Nano* 13 (4) (2019) 3847–3857.
- [124] F. Wang et al., Flexible wearable graphene/alginate composite non-woven fabric temperature sensor with high sensitivity and anti-interference, *Cellulose* 27 (4) (2020) 2369–2380.
- [125] D. Wu, F. Zhang, H. Liang, X. Feng, Nanocomposites and macroscopic materials: assembly of chemically modified graphene sheets, *Chem. Soc. Rev.* 41(18) (2012) 6160–6177. doi: 10.1039/C2CS35179J.
- [126] X. Gong, L. Zhang, Y. Huang, S. Wang, G. Pan, L. Li, Directly writing flexible temperature sensor with graphene nanoribbons for disposable healthcare devices, *RSC Adv.* 10 (37) (2020) 22222–22229.
- [127] A.M. Soomro, F. Jabbar, M. Ali, J.-W. Lee, S.W. Mun, K.H. Choi, All-range flexible and biocompatible humidity sensor based on poly lactic glycolic acid (PLGA) and its application in human breathing for wearable health monitoring, *J. Mater. Sci.: Mater. Electron.* 30 (10) (2019) 9455–9465.
- [128] Q. Fu, C. Cui, L. Meng, S. Hao, R. Dai, J. Yang, Emerging cellulose-derived materials: a promising platform for the design of flexible wearable sensors toward health and environment monitoring, *Mater. Chem. Front.* 5 (5) (2021) 2051–2091.
- [129] J. Zhang et al., Highly transparent, self-healing, injectable and self-adhesive chitosan/polyzwitterion-based double network hydrogel for potential 3D printing wearable strain sensor, *Mater. Sci. Eng., C* 117 (2020) 111298.
- [130] S. Harada, K. Kanao, Y. Yamamoto, T. Arie, S. Akita, K. Takei, Fully printed flexible fingerprint-like three-axis tactile and slip force and temperature sensors for artificial skin, *ACS Nano* 8 (12) (2014) 12851–12857.
- [131] C.-Y. Lee et al., Use of flexible micro-temperature sensor to determine temperature in situ and to simulate a proton exchange membrane fuel cell, *J. Power Sources* 196 (1) (2011) 228–234, <https://doi.org/10.1016/j.jpowsour.2010.06.051>.
- [132] D. Barmpakos, C. Tsamis, G. Kaltsas, Multi-parameter paper sensor fabricated by inkjet-printed silver nanoparticle ink and PEDOT:PSS, *Microelectron. Eng.* 225 (2020) 111266, <https://doi.org/10.1016/j.mee.2020.111266>.
- [133] V.S. Turkani et al., Nickel based RTD fabricated via additive screen printing process for flexible electronics, *IEEE Access* 7 (2019) 37518–37527, <https://doi.org/10.1109/ACCESS.2019.2904970>.
- [134] P. Sehrawat, S.S. Abid, P.M. Islam, M. Khanuja, A multi-prong approach towards the development of high performance temperature sensor using MWCNTs/Al₂O₃ composite film, *Mater. Res. Bull.* 99 (2018) 1–9, <https://doi.org/10.1016/j.materresbull.2017.10.045>.
- [135] S.Y. Hong et al., Stretchable active matrix temperature sensor array of polyaniline nanofibers for electronic skin, *Adv. Mater.* 28 (5) (2016) 930–935.
- [136] S.V. Grayli, G.W. Leach, B. Bahreyni, Sol-gel deposition and characterization of vanadium pentoxide thin films with high TCR, *Sens. Actuat., A* 279 (2018) 630–637, <https://doi.org/10.1016/j.sna.2018.07.002>.
- [137] Z.-Y. Yan, J.-Y. Liu, J.-R. Niu, Research of a novel Ag temperature sensor based on fabric substrate fabricated by magnetron sputtering, *Materials* 14(20) (2021). doi: 10.3390/ma14206014.
- [138] S. Sarma, J.H. Lee, Developing efficient thin film temperature sensors utilizing layered carbon nanotube films, *Sensors* 18(10) (2018). doi: 10.3390/s18103182.
- [139] C. Fay et al., Wireless ion-selective electrode autonomous sensing system, *IEEE Sens. J.* 11 (10) (2011) 2374–2382.
- [140] R. Lu et al., A low-power sensitive integrated sensor system for thermal flow monitoring, *IEEE Trans. Very Large Scale Integr. VLSI Syst.* 27 (12) (2019) 2949–2953.
- [141] R. Kumar, X. Liu, J. Zhang, M. Kumar, Room-temperature gas sensors under photoactivation: from metal oxides to 2D materials, *Nano-Micro Lett.* 12 (1) (2020) 1–37.
- [142] Q. Jiang et al., Highly sensitive, low voltage operation, and low power consumption resistive strain sensors based on vertically oriented graphene nanosheets, *Adv. Mater. Technol.* 4 (3) (2019) 1800572.
- [143] E. Kovalska, A. Baldycheva, A. Somov, Wireless graphene-enabled wearable temperature sensor, in: *Journal of Physics: Conference Series*, vol. 1571(1), IOP Publishing, 2020, p. 012001.

- [144] A. Somov, E. Kovalska, A. Baldycheva, Wireless graphene temperature sensor, in: 2020 IEEE Sensors, 2020, IEEE, pp. 1–4.
- [145] J.S. Chaglla, E.N. Celik, W. Balachandran, Measurement of core body temperature using graphene-inked infrared thermopile sensor, *Sensors* 18 (10) (2018) 3315.
- [146] C. Zhou, X. Zhang, H. Zhang, X. Duan, Temperature sensing at the robot fingertip using reduced graphene oxide-based sensor on a flexible substrate, in: IEEE SENSORS, IEEE, 2019, pp. 1–4.
- [147] M. Potenza, A. Cataldo, G. Bovesecchi, S. Corasaniti, P. Coppa, S. Bellucci, Graphene nanoplatelets: thermal diffusivity and thermal conductivity by the flash method, *AIP Adv.* 7 (7) (2017) 075214.
- [148] K. Gouda, S. Bhowmik, B. Das, Thermomechanical behavior of graphene nanoplatelets and bamboo micro filler incorporated epoxy hybrid composites, *Mater. Res. Express* 7 (1) (2020) 015328.
- [149] C.N. Lau, W. Bao, J. Velasco Jr, Properties of suspended graphene membranes, *Mater. Today* 15 (6) (2012) 238–245.
- [150] N.M. Julkapli, S. Bagheri, S. Sapuan, Multifunctionalized carbon nanotubes polymer composites: properties and applications, in: *Eco-friendly Polymer Nanocomposites*, Springer, 2015, pp. 155–214.
- [151] E. Omanović-Miklićanin, A. Badnjević, A. Kazlagić, M. Hajlovac, Nanocomposites: a brief review, *Health Technol.* (2019) 1–9.
- [152] K.E. Whitener, P.E. Sheehan, Graphene synthesis, *Diam. Relat. Mater.* 46 (2014) 25–34, <https://doi.org/10.1016/j.diamond.2014.04.006>.
- [153] H. Souri, D. Bhattacharyya, Highly stretchable multifunctional wearable devices based on conductive cotton and wool fabrics, *ACS Appl. Mater. Interfaces* 10 (24) (2018) 20845–20853, <https://doi.org/10.1021/acsami.8b04775>.
- [154] H. Souri, D. Bhattacharyya, Wearable strain sensors based on electrically conductive natural fiber yarns, *Mater. Des.* 154 (2018) 217–227, <https://doi.org/10.1016/j.matdes.2018.05.040>.
- [155] H. Souri, D. Bhattacharyya, Wool fabrics decorated with carbon-based conductive ink for low-voltage heaters, *Mater. Adv.* 3 (9) (2022) 3952–3960, <https://doi.org/10.1039/D1MA00981H>.
- [156] F. Marra, S. Minutillo, A. Tamburrano, M.S. Sarto, Production and characterization of graphene nanoplatelet-based ink for smart textile strain sensors via screen printing technique, *Mater. Des.* 198 (2021) 109306.
- [157] D.H. Ho, Q. Sun, S.Y. Kim, J.T. Han, D.H. Kim, J.H. Cho, Stretchable and multimodal all graphene electronic skin, *Adv. Mater.* 28 (13) (2016) 2601–2608.
- [158] Y. Qiao et al., Substrate-free multilayer graphene electronic skin for intelligent diagnosis, *ACS Appl. Mater. Interf.* 12 (44) (2020) 49945–49956.
- [159] H. Souri, D. Bhattacharyya, Highly sensitive, stretchable and wearable strain sensors using fragmented conductive cotton fabric, *J. Mater. Chem. C* 6(39) (2018) 10524–10531. doi: 10.1039/C8TC03702G.
- [160] V. Shirhatti, S. Nuthalapati, V. Kedambaimoole, S. Kumar, M.M. Nayak, K. Rajanna, Multifunctional graphene sensor ensemble as a smart biomonitoring fashion accessory, *ACS Sens.* 6 (12) (2021) 4325–4337, <https://doi.org/10.1021/acssensors.1c01393>.
- [161] R. Fang, R. Song, X. Zhao, Z. Wang, W. Qian, D. He, Compact and low-profile UWB antenna based on graphene-assembled films for wearable applications, *Sensors* 20(9) (2020) 2552. <<https://www.mdpi.com/1424-8220/20/9/2552>>.
- [162] Z. Wang et al., High conductive graphene assembled films with porous microstructure for freestanding and ultra-low power strain sensors, *Sci. Bull.* 65 (16) (2020/08/30/ 2020,) 1363–1370, <https://doi.org/10.1016/j.scib.2020.05.002>.
- [163] J. Zhang et al., “Flexible graphene-assembled film-based antenna for wireless wearable sensor with miniaturized size and high sensitivity,” (in eng), *ACS Omega* 5 (22) (2020) 12937–12943, <https://doi.org/10.1021/acsomega.0c00263>.
- [164] N.K. Mogha, V. Sahu, M. Sharma, R.K. Sharma, D.T. Masram, Biocompatible ZrO₂- reduced graphene oxide immobilized AChE biosensor for chlorpyrifos detection, *Mater. Des.* 111 (2016/12/05/ 2016,) 312–320, <https://doi.org/10.1016/j.matdes.2016.09.019>.